Atmos. Chem. Phys. Discuss., 15, 32005–32047, 2015
www.atmos-chem-phys-discuss.net/15/32005/2015/
doi:10.5194/acpd-15-32005-2015

Atmospheric Chemistry and Physics Discussions

Aqueous-phase mechanism for secondary organic aerosol formation from isoprene: application to the Southeast United States and co-benefit of SO_2 emission controls

E. A. Marais[1], D. J. Jacob[1,2], J. L. Jimenez[3,4], P. Campuzano-Jost[3,4], D. A. Day[3,4], W. Hu[3,4], J. Krechmer[3,4], L. Zhu[1], P. S. Kim[2], C. C. Miller[2], J. A. Fisher[5], K. Travis[1], K. Yu[1], T. F. Hanisco[6], G. M. Wolfe[6,7], H. L. Arkinson[8], H. O. T. Pye[9], K. D. Froyd[3,10], J. Liao[3,10], and V. F. McNeill[11]

[1]School of Engineering and Applied Sciences, Harvard University, Cambridge, MA, USA
[2]Earth and Planetary Sciences, Harvard University, Cambridge, MA, USA
[3]Cooperative Institute for Research in Environmental Sciences, University of Colorado, Boulder, CO, USA
[4]Department of Chemistry and Biochemistry, University of Colorado, Boulder, CO, USA
[5]School of Chemistry and School of Earth and Environmental Sciences, University of Wollongong, Wollongong, New South Wales, Australia

[6]Atmospheric Chemistry and Dynamics Lab, NASA Goddard Space Flight Center, Greenbelt, MD, USA
[7]Joint Center for Earth Systems Technology, University of Maryland Baltimore County, Baltimore, MD, USA
[8]Department of Atmospheric and Oceanic Science, University of Maryland, College Park, MD, USA
[9]National Exposure Research Laboratory, US EPA, Research Triangle Park, NC, USA
[10]Chemical Sciences Division, Earth System Research Laboratory, NOAA, Boulder, Colorado, USA
[11]Department of Chemical Engineering, Columbia University, New York, NY 10027, USA

Received: 21 October 2015 – Accepted: 30 October 2015 – Published: 13 November 2015

Correspondence to: E. A. Marais (emarais@seas.harvard.edu)

Published by Copernicus Publications on behalf of the European Geosciences Union.

ACPD
15, 32005–32047, 2015

Abstract

Isoprene emitted by vegetation is an important precursor of secondary organic aerosol (SOA), but the mechanism and yields are uncertain. Aerosol is prevailingly aqueous under the humid conditions typical of isoprene-emitting regions. Here we develop an aqueous-phase mechanism for isoprene SOA formation coupled to a detailed gas-phase isoprene oxidation scheme. The mechanism is based on aerosol reactive uptake probabilities (γ) for water-soluble isoprene oxidation products, including sensitivity to aerosol acidity and nucleophile concentrations. We apply this mechanism to simulation of aircraft (SEAC^{4}RS) and ground-based (SOAS) observations over the Southeast US in summer 2013 using the GEOS-Chem chemical transport model. Emissions of nitrogen oxides ($NO_x \equiv NO + NO_2$) over the Southeast US are such that the peroxy radicals produced from isoprene oxidation ($ISOPO_2$) react significantly with both NO (high-NO_x pathway) and HO_2 (low-NO_x pathway), leading to different suites of isoprene SOA precursors. We find a mean SOA mass yield of 3.3 % from isoprene oxidation, consistent with the observed relationship of OA and formaldehyde (a product of isoprene oxidation). The yield is mainly contributed by two immediate gas-phase precursors, isoprene epoxydiols (IEPOX, 58 % of isoprene SOA) from the low-NO_x pathway and glyoxal (28 %) from both low- and high-NO_x pathways. This speciation is consistent with observations of IEPOX SOA from SOAS and SEAC^{4}RS. Observations show a strong relationship between IEPOX SOA and sulfate aerosol that we explain as due to the indirect effect of sulfate on aerosol acidity and volume, rather than a direct mechanistic role for sulfate. Isoprene SOA concentrations increase as NO_x emissions decrease (favoring the low-NO_x pathway for isoprene oxidation), but decrease as SO_2 emissions decrease (due to the effect of sulfate on aerosol acidity and volume). The US EPA projects 2013–2025 decreases in anthropogenic emissions of 34 % for NO_x (leading to 7 % increase in isoprene SOA) and 48 % for SO_2 (35 % decrease in isoprene SOA). The combined projected decreases in NO_x and SO_2 emissions reduce isoprene SOA yields from 3.3 to 2.3 %. Reducing SO_2 emissions decreases sulfate and isoprene

ACPD
15, 32005–32047, 2015

SOA by a similar magnitude, representing a factor of 2 co-benefit for $PM_{2.5}$ from SO_2 emission controls.

1 Introduction

Isoprene emitted by vegetation is a major source of secondary organic aerosol (SOA) (Carlton et al., 2009 and references therein) with effects on human health, visibility, and climate. There is large uncertainty in the yield and composition of isoprene SOA (Scott et al., 2014; McNeill et al., 2014), involving a cascade of species produced in the gas-phase oxidation of isoprene and their interaction with pre-existing aerosol (Hallquist et al., 2009). We develop here a new aqueous-phase mechanism for isoprene SOA formation coupled to gas-phase chemistry, implement it in the GEOS-Chem chemical transport model (CTM) to simulate observations in the Southeast US, and from there derive new constraints on isoprene SOA yields and the contributing pathways.

Organic aerosol is ubiquitous in the atmosphere, often dominating fine aerosol mass (Zhang et al., 2007), including in the Southeast US where it accounts for more than 60 % in summer (Attwood et al., 2014). It may be directly emitted by combustion as primary organic aerosol (POA), or produced within the atmosphere as SOA by oxidation of volatile organic compounds (VOCs). Isoprene (C_5H_8) from vegetation is the dominant VOC emitted globally, and the Southeast US in summer is one of the largest isoprene-emitting regions in the world (Guenther et al., 2006). SOA yields from isoprene are low compared with larger VOCs (Pye et al., 2010), but isoprene emissions are much higher. Kim et al. (2015) estimated that isoprene accounts for 40 % of total organic aerosol in the Southeast US in summer.

Formation of OA from oxidation of isoprene depends on local concentrations of nitrogen oxide radicals ($NO_x \equiv NO + NO_2$) and pre-existing aerosol. NO_x concentrations determine the fate of organic peroxy radicals originating from isoprene oxidation ($ISOPO_2$), leading to different cascades of oxidation products in the low-NO_x and high-NO_x pathways (Paulot et al., 2009a, b). Uptake of isoprene oxidation products to the

ACPD
15, 32005–32047, 2015

aerosol phase depends on their vapor pressure (Donahue et al., 2006), solubility in aqueous media (Saxena and Hildeman, 1996), and subsequent condensed-phase reactions (Volkamer et al., 2007). Aqueous aerosol provides a medium for reactive uptake (Eddingsaas et al., 2010; Surratt et al., 2010) with dependences on acidity (Surratt et al., 2007b), concentration of nucleophiles such as sulfate (Surratt et al., 2007a), aerosol water (Carlton and Turpin, 2013), and organic coatings (Gaston et al., 2014).

We compile in Fig. 1 the published laboratory yields of isoprene SOA as a function of initial NO concentration and relative humidity (RH). Here and elsewhere, the isoprene SOA yield is defined as the mass of SOA produced per unit mass of isoprene oxidized. Isoprene SOA yields span a wide range, from $< 0.1\,\%$ to $> 10\,\%$, with no systematic difference between low-NO_x and high-NO_x pathways. Yields tend to be higher in dry chambers (RH $< 10\,\%$). Under such dry conditions, aerosol formation likely involves reversible partitioning of semivolatile isoprene oxidation products into the organic aerosol phase (Virtanen et al., 2010; Song et al., 2015). At humid conditions more representative of the atmosphere, aerosols are aqueous and the mechanisms for uptake may be different (Virtanen et al., 2010). Standard isoprene SOA mechanisms used in atmospheric models assume reversible partitioning onto pre-existing organic aerosol, fitting the dry chamber data (Odum et al., 1996). However, this may not be appropriate for actual atmospheric conditions where aqueous-phase chemistry with irreversible reactive uptake of water-soluble gases is likely the dominant mechanism (Ervens et al., 2011; Carlton and Turpin, 2013).

Here we present a mechanism for irreversible aqueous-phase isoprene SOA formation integrated within a detailed chemical mechanism for isoprene gas-phase oxidation, thus linking isoprene SOA formation to gas-phase chemistry and avoiding more generic volatility-based parameterizations that assume dry organic aerosol (Odum et al., 1996; Donahue et al., 2006). We use this mechanism in the GEOS-Chem CTM to simulate observations from the SOAS (surface) and SEAC^{4}RS (aircraft) field campaigns over the Southeast US in summer 2013, with focus on isoprene SOA components and on the relationship between OA and formaldehyde (HCHO). HCHO is a high-yield oxida-

ACPD
15, 32005–32047, 2015

tion product of isoprene (Palmer et al., 2003) and we use the OA-HCHO relationship as a constraint on isoprene SOA yields. SOAS measurements were made at a ground site in rural Centreville, Alabama (Hu et al., 2015; http://soas2013.rutgers.edu/). SEAC^{4}RS measurements were made from the NASA DC-8 aircraft with extensive boundary layer coverage across the Southeast (Toon et al., 2015; SEAC^{4}RS Archive).

2 Chemical mechanism for isoprene SOA formation

The previous default treatment of isoprene SOA in GEOS-Chem (v9-02; http://geos-chem.org) follows a standard parameterization that operates independently from the gas-phase chemistry mechanism and is based on reversible partitioning onto pre-existing OA of generic semivolatile products of isoprene oxidation by OH and NO_3 radicals (Pye et al., 2010). Here we implement a new mechanism for irreversible uptake by aqueous aerosols of species produced in the isoprene oxidation cascade of the GEOS-Chem gas-phase mechanism. This couples SOA formation to the gas-phase chemistry and is in accord with increased evidence for a major role of aqueous aerosols in isoprene SOA formation (Ervens et al., 2011).

The standard gas-phase isoprene oxidation mechanism in GEOS-Chem v9-02 is described in Mao et al. (2013) and is based on best knowledge at the time building on mechanisms for the oxidation of isoprene by OH (Paulot et al., 2009a, b) and NO_3 (Rollins et al., 2009). Updates implemented in this work are described below and in companion papers applying GEOS-Chem to simulation of observed gas-phase isoprene oxidation products over the Southeast US in summer 2013 (Fisher et al., 2015; Travis et al., 2015). Most gas-phase products of the isoprene oxidation cascade in GEOS-Chem have high dry deposition velocity, competing in some cases with removal by oxidation and aerosol formation (Nguyen et al., 2015b; Travis et al., 2015).

Figure 2 shows the isoprene oxidation cascade in GEOS-Chem leading to SOA formation. Reaction pathways leading to isoprene SOA precursors are described below. Yields are in mass percent, unless stated otherwise. Reactive $ISOPO_2$ isomers formed

ACPD
15, 32005–32047, 2015

in the first OH oxidation step react with NO, the hydroperoxyl radical (HO_2), other peroxy radicals (RO_2), or undergo isomerization (Peeters et al., 2009). The NO reaction pathway (high-NO_x pathway) yields C_5 hydroxy carbonyls, methyl vinyl ketone, methacrolein, and first-generation isoprene nitrates (ISOPN). The first three products go on to produce glyoxal and methylglyoxal, which serve as SOA precursors. The overall yield of glyoxal from the high-NO_x pathway is 7 mol %. Oxidation of ISOPN by OH and O_3 is as described by Lee et al. (2014). Reaction of ISOPN with OH produces saturated dihydroxy dinitrates (DHDN), 21 and 27 mol % from the beta and delta channels respectively (Lee et al., 2014), and 10 mol % isoprene epoxydiols (IEPOX) from each channel (Jacobs et al., 2014). We also adopt the mechanism of Lin et al. (2013) to generate C_4 hydroxyepoxides (methacrylic acid epoxide and hydroxymethylmethyl-α-lactone, both denoted MEPOX) from OH oxidation of a peroxyacylnitrate formed when methacrolein reacts with OH followed by NO_2. Only hydroxymethylmethyl-α-lactone is shown in Fig. 2.

The HO_2 reaction pathway for $ISOPO_2$ leads to formation of hydroxyhydroperoxides (ISOPOOH) that are oxidized to IEPOX (Paulot et al., 2009b) and several low-volatility products, represented here as C_5-LVOC (Krechmer et al., 2015). The kinetics of IEPOX oxidation by OH is uncertain, and experimentally determined IEPOX lifetimes vary from 8 to 28 h for an OH concentration of 1×10^6 molecules cm^{-3} (Jacobs et al., 2013; Bates et al., 2014). In GEOS-Chem we apply the fast kinetics of Jacobs et al. (2013) and reduce the yield of IEPOX from ISOPOOH from 100 to 75 %, within the range observed by St. Clair et al. (2015), to address a factor of 4 overestimate in simulated IEPOX (Nguyen et al., 2015b). IEPOX oxidizes to form glyoxal and methylglyoxal (Bates et al., 2014). The overall glyoxal yield from the $ISOPO_2 + HO_2$ pathway is 6 mol %. Krechmer et al. (2015) report a 2.5 mol % yield of C_5-LVOC from ISOPOOH but we reduce this to 0.5 mol % to reproduce surface observations of the corresponding aerosol products (Sect. 4). Methyl vinyl ketone and methacrolein yields from the $ISOPO_2 + HO_2$ pathway are 2.5 and 3.8 mol %, respectively (Liu et al., 2013), sufficiently low that they do not lead to significant SOA formation.

ACPD
15, 32005–32047, 2015

Minor channels for $ISOPO_2$ are isomerization and reaction with RO_2. Isomerization forms hydroperoxyaldehydes (HPALD) that go on to photolyze, but products are uncertain (Peeters and Müller, 2010). We assume 25 mol % yield each of glyoxal and methylglyoxal from HPALD photolysis in GEOS-Chem following Stavrakou et al. (2010). Reaction of $ISOPO_2$ with RO_2 leads to the same suite of C_4-C_5 carbonyls as reaction with NO (C_5 hydroxy carbonyls, methacrolein, and methyl vinyl ketone) and from there to glyoxal and methylglyoxal.

Immediate aerosol precursors from the isoprene +OH oxidation cascade are identified in Fig. 2. For the high-NO_x pathway ($ISOPO_2 + NO$ channel) precursors include glyoxal and methylglyoxal (McNeill et al., 2012), ISOPN (Darer et al., 2011; Hu et al., 2011), DHDN (Lee et al., 2014), MEPOX (Lin et al., 2013), and IEPOX (Jacobs et al., 2014). For the low-NO_x pathway ($ISOPO_2 + HO_2$ channel) they include IEPOX (Eddingsaas et al., 2010), C_5-LVOC (Krechmer et al., 2015, in which the aerosol-phase species is denoted ISOPOOH-SOA), glyoxal, and methylglyoxal. Glyoxal and methylglyoxal are also produced from the $ISOPO_2 + RO_2$ and $ISOPO_2$ isomerization channels.

Ozonolysis and oxidation by NO_3 are additional minor isoprene reaction pathways (Fig. 2). The NO_3 oxidation pathway is a potentially important source of isoprene SOA at night (Brown et al., 2009) from the irreversible uptake of low-volatility second-generation hydroxynitrates (NT-ISOPN) (Ng et al., 2008; Rollins et al., 2009). We update the gas-phase chemistry of Rollins et al. (2009), implemented by Mao et al. (2013), to include formation of 4 mol % of the aerosol-phase precursor NT-ISOPN from first-generation alkylnitrates (Rollins et al., 2009). Ozonolysis products are volatile and observed SOA yields in chamber studies are low (< 1 %; Kleindienst et al., 2007). In GEOS-Chem only methylglyoxal is an aerosol precursor from isoprene ozonolysis.

We implement irreversible uptake of isoprene oxidation products to aqueous aerosols using laboratory-derived reactive uptake probabilities (γ) as given by Anttila

ACPD
15, 32005–32047, 2015

et al. (2006) and Gaston et al. (2014):

$$\gamma = \left[\frac{1}{\alpha} + \frac{3\omega}{4rRTH^{*}k_{aq}}\right]^{-1}. \quad (1)$$

Here α is the mass accommodation coefficient (taken as 0.1 for all immediate SOA precursors in Fig. 2), ω is the mean gas-phase molecular speed ($cm\,s^{-1}$), r is the aqueous particle radius (cm), R is the universal gas constant ($0.08206\,L\,atm\,K^{-1}\,mol^{-1}$), T is temperature (K), H^{*} is the effective Henry's Law constant ($M\,atm^{-1}$) accounting for any fast dissociation equilibria in the aqueous phase, and k_{aq} is the pseudo first-order aqueous-phase reaction rate constant (s^{-1}) for conversion to non-volatile products.

Precursors with epoxide functionality, IEPOX and MEPOX, undergo acid-catalyzed epoxide ring opening and nucleophilic addition in the aqueous phase. The aqueous-phase reaction rate constant is from Eddingsaas et al. (2010),

$$k_{aq} = k_{H^+}[H^+] + k_{nuc}[nuc][H^+] + k_{HSO_4^-}\left[HSO_4^-\right], \quad (2)$$

and includes three channels: acid-catalyzed ring opening followed by nucleophilic addition of H_2O (k_{H^+} in $M^{-1}\,s^{-1}$), acid-catalyzed ring opening followed by nucleophilic addition of sulfate and nitrate ions ($nuc \equiv SO_4^{2-} + NO_3^-$, k_{nuc} in $M^{-2}\,s^{-1}$), and concerted protonation and nucleophilic addition by bisulfate, HSO_4^- ($k_{HSO_4^-}$ in $M^{-1}\,s^{-1}$). Reaction rate constants in the literature are from experiments in concentrated media, representative of aqueous aerosols, so no activity correction factors are used in our work.

Precursors with nitrate functionality (-ONO_2), ISOPN and DHDN, hydrolyze to form low-volatility polyols and nitric acid (Hu et al., 2011; Jacobs et al., 2014), so k_{aq} in Eq. (1) is the hydrolysis rate constant.

Glyoxal and methylglyoxal form SOA irreversibly by surface uptake followed by aqueous-phase oxidation and oligomerization to yield non-volatile products (Liggio et al., 2005; Volkamer et al., 2009; Nozière et al., 2009; Ervens et al., 2011; Knote

ACPD
15, 32005–32047, 2015

et al., 2014). Glyoxal forms SOA with higher yields during the day than at night due to OH aqueous-phase chemistry (Tan et al., 2009; Volkamer et al., 2009; Summer et al., 2014). We use a daytime γ of 2.9×10^{-3} for glyoxal from Liggio et al. (2005) and a nighttime γ of 5×10^{-6} (Waxman et al., 2013; Sumner et al., 2014). The SOA yield of methylglyoxal is small compared with that of glyoxal (McNeill et al., 2012). A previous GEOS-Chem study by Fu et al. (2008) used the same γ (2.9×10^{-3}) for glyoxal and methylglyoxal. Reaction rate constants are similar for aqueous-phase processing of glyoxal and methylglyoxal (Buxton et al., 1997; Ervens et al., 2003), but H^* of glyoxal is about 4 orders of magnitude higher. Here we scale the γ for methylglyoxal to the ratio of effective Henry's law constants: $H^* = 3.7 \times 10^3\,\mathrm{M\,atm^{-1}}$ for methylglyoxal (Tan et al., 2010) and $H^* = 2.7 \times 10^7\,\mathrm{M\,atm^{-1}}$ for glyoxal (Sumner et al., 2014). The resulting uptake of methylglyoxal is very slow and makes a negligible contribution to isoprene SOA.

The aerosol precursors C_5-LVOC from ISOPOOH oxidation and NT-ISOPN from isoprene reaction with NO_3 have low volatility and are assumed to condense to aerosols with a γ of 0.1 limited by mass accommodation.

Table 1 gives input variables used to calculate γ for IEPOX, ISOPN, and DHDN by Eqs. (1) and (2). Table 2 lists average values of γ for all immediate aerosol precursors in the Southeast US boundary layer in summer as simulated by GEOS-Chem (Sect. 3). γ for IEPOX is a strong function of pH and increases linearly from 1×10^{-4} to 1×10^{-2} as pH decreases from 3 to 0. We obtain values of γ for MEPOX by reducing IEPOX γ by a factor of 30 when the aerosol is acidic (pH < 4), due to slower acid-catalyzed ring opening (Piletic et al., 2013; Riedel et al., 2015). At pH > 4 we assume that γ for IEPOX and MEPOX are the same (Riedel et al., 2015), but they are then very low.

We neglect isoprene SOA formation in clouds because the aqueous-phase concentrations and acidities are too low for most of the above aqueous-phase mechanisms to take place at a significant rate. Observations show that the isoprene SOA yield in the presence of laboratory-generated clouds is very low (0.2–0.4 %; Brégonzio-Rozier et al., 2015). Wagner et al. (2015) found no significant production of SOA in the shal-

ACPD
15, 32005–32047, 2015

low convective cloud layer (1–2 km altitude) over the Southeast US during SEAC^{4}RS, supporting our assumption that this pathway is minor.

3 GEOS-Chem simulation and isoprene SOA yields

Several companion papers apply GEOS-Chem to interpret SEAC^{4}RS and surface data over the Southeast US in summer 2013 including Kim et al. (2015) for aerosols, Fisher et al. (2015) for organic nitrates, Travis et al. (2015) for ozone and NO_x, and Zhu et al. (2015) for validation of satellite HCHO data. These studies use a model version with $0.25^\circ \times 0.3125^\circ$ horizontal resolution over North America, nested within a $4^\circ \times 5^\circ$ global simulation. Here we use a $2^\circ \times 2.5^\circ$ global GEOS-Chem simulation with no nesting. Yu et al. (2015) found little difference between $0.25^\circ \times 0.3125^\circ$ and $2^\circ \times 2.5^\circ$ resolutions in simulated regional statistics for isoprene chemistry.

The reader is referred to Kim et al. (2015) for a general presentation of the model including evaluation with Southeast US aerosol observations, and to Travis et al. (2015) and Fisher et al. (2015) for presentation of gas-phase chemistry and comparisons with observed gas-phase isoprene oxidation products. Isoprene emission is from the MEGAN v2.1 inventory (Guenther et al., 2012). The companion papers decrease isoprene emission by 15 % from the MEGAN v2.1 values to fit the HCHO data (Zhu et al., 2015), but this is not applied here.

Our OA simulation differs in several ways from that of Kim et al. (2015). They assumed a fixed 3 % yield of isoprene SOA. The aqueous-phase mechanism coupled to gas-phase isoprene chemistry described in Sect. 2, replacing the semivolatile reversible partitioning scheme of Pye et al. (2010), is original to this work. Our resulting mean isoprene SOA yield for the Southeast US (3.3 %, discussed below) turns out to be consistent with that assumed by Kim et al. (2015). Kim et al. (2015) included parameterizations for formation of anthropogenic and open fire SOA (Hodzic and Jimenez, 2011) but these are not included here. They presented detailed comparisons to total OA measurements from SEAC^{4}RS and from surface networks, finding no systematic

ACPD
15, 32005–32047, 2015

bias. Our omission of anthropogenic and open fire SOA leads to some underestimation of total OA, as will be discussed below.

Organic aerosol and sulfate contribute most of the aerosol mass over the Southeast US in summer, while nitrate is much lower (Kim et al., 2015). GEOS-Chem uses the ISORROPIA thermodynamic model (Fountoukis and Nenes, 2007) to simulate sulfate-nitrate-ammonium (SNA) aerosol composition, water content, and acidity as a function of local conditions. Simulated aerosol pH along the SEAC^{4}RS flight tracks in the Southeast US boundary layer averages 1.3 (interquartiles 0.92 and 1.8). The aerosol pH remains below 3 even when sulfate aerosol is fully neutralized by ammonia (Guo et al., 2015).

The rate of gas uptake by the aqueous aerosol is computed with the pseudo-first order reaction rate constant k_{het} (s^{-1}) (Schwartz, 1986; Jacob, 2000):

$$k_{het} = \int_0^\infty 4\pi r^2 \left(\frac{r}{D_g} + \frac{4}{\gamma \omega} \right)^{-1} n(r) \mathrm{d}r, \quad (3)$$

where D_g is the gas-phase diffusion constant (taken to be 0.1 cm^2 s^{-1}) and $n(r)$ is the number size distribution of aqueous aerosol (cm^{-4}). We take $n(r)$ to be the size distribution of sulfate aerosol, making the assumption that all aqueous particles would contain some sulfate. Clear-sky RH in the Southeast US boundary layer during SEAC^{4}RS averaged 72 ± 17 %, sufficiently high that sulfate aerosol is expected to be aqueous under all conditions (Wang et al., 2008).

The sulfate aerosol size distribution including RH-dependent hygroscopic growth factors is from the Global Aerosol Data Set (GADS) of Koepke et al. (1997), as originally implemented in GEOS-Chem by Martin et al. (2003) and updated by Drury et al. (2010). The GADS size distribution compares well with observations over the eastern US in summer (Drury et al., 2010), including for SEAC^{4}RS (Kim et al., 2015). We compute $n(r)$ locally in GEOS-Chem by taking the dry SNA mass concentration, converting from mass to volume with a dry aerosol mass density of 1700 kg m^{-3} (Hess et al.,

ACPD
15, 32005–32047, 2015

1998), applying the aerosol volume to the dry sulfate size distribution in GADS, and then applying the GADS hygroscopic growth factors. We verified that the hygroscopic growth factors from GADS agree within 10 % with those computed locally from ISORROPIA.

Figure 2 shows the mean branching ratios for isoprene oxidation in the Southeast US boundary layer as calculated by GEOS-Chem. 87 % of isoprene reacts with OH, 8 % with ozone, and 5 % with NO_3. Oxidation of isoprene by OH produces $ISOPO_2$ of which 51 % react with NO (high-NO_x pathway), 35 % react with HO_2, 8 % isomerize, and 6 % react with other RO_2 radicals.

Glyoxal is an aerosol precursor common to all isoprene + OH pathways in our mechanism with yields of 7 mol % from the $ISOPO_2 + NO$ pathway, 6 mol % from $ISOPO_2 + HO_2$, 11 mol % from $ISOPO_2 + RO_2$, and 25 mol % from $ISOPO_2$ isomerization. For the Southeast US conditions we thus find that 44 % of glyoxal is from the $ISOPO_2 + NO$ pathway, 24 % from $ISOPO_2 + HO_2$, 8 % from $ISOPO_2 + RO_2$, and 24 % from $ISOPO_2$ isomerization.

The mean total yield of isoprene SOA computed in GEOS-Chem for the Southeast US boundary layer is 3.3 %, as shown in Fig. 2. IEPOX contributes 1.9 % and glyoxal 0.9 %. The low-NO_x pathway involving $ISOPO_2$ reaction with HO_2 contributes 73 % of the total isoprene SOA yield, mostly from IEPOX, even though this pathway is only 35 % of the fate of $ISOPO_2$. The high-NO_x pathway contributes 16 % of isoprene SOA, mostly from glyoxal. MEPOX contribution to isoprene SOA is small (2 %) and consistent with a recent laboratory study that finds low SOA yields from this pathway under humid conditions (Nguyen et al., 2015a). The minor low-NO_x pathways from $ISOPO_2$ isomerization and reaction with RO_2 contribute 8 % of isoprene SOA through glyoxal. The remainder of isoprene SOA formation (3 %) is from nighttime oxidation by NO_3.

The dominance of IEPOX and glyoxal as precursors for isoprene SOA was previously reported by McNeill et al. (2012) using a photochemical box model. Both of these precursors are produced photochemically, and both are also removed photochemically in the gas phase by reaction with OH (and photolysis for glyoxal). The mean lifetimes

ACPD
15, 32005–32047, 2015

of IEPOX and glyoxal against gas-phase photochemical loss average 1.6 and 2.3 h respectively for SEAC^{4}RS daytime conditions; mean lifetimes against reactive uptake by aerosol are 31 and 20 h, respectively. For both species, aerosol uptake is a minor sink competing with gas-phase photochemical loss. The model boundary-layer yield of IEPOX SOA from IEPOX is 5 %, consistent with average yields from chamber experiments (4–10 %) for aerosols with similar acidity to aerosols in the Southeast US (Riedel et al., 2015).

The dominance of gas-phase loss over aerosol uptake for both IEPOX and glyoxal implies that isoprene SOA formation is highly sensitive to their reactive uptake probabilities γ and to the aqueous aerosol mass concentration (in both cases, γ is small enough that uptake is controlled by bulk aqueous-phase rather than surface reactions). We find under SEAC^{4}RS conditions that γ for IEPOX is mainly controlled by aerosol free acidity ($k_{H+}[H^+]$ in Eq. 2), with little contribution from nucleophile-driven and HSO_4^--driven channels. This will be discussed below in comparing to SOAS and SEAC^{4}RS observations.

The 3.3 % mean yield of isoprene SOA from our mechanism is consistent with the fixed yield of 3 % assumed by Kim et al. (2015) in their GEOS-Chem simulation of the SEAC^{4}RS period, including extensive comparisons to OA observations that showed a 40 % mean contribution of isoprene to total OA. We conducted a sensitivity simulation using the default isoprene SOA mechanism in GEOS-Chem based on reversible partitioning of semivolatile oxidation products onto pre-existing OA (Pye et al., 2010). The isoprene SOA yield in that simulation was only 1.1 %. The observed correlation of OA with HCHO in SEAC^{4}RS supports our higher yield, as shown below.

4 Evaluation with observational constraints on isoprene SOA

Isoprene is the largest source of HCHO in the Southeast US (Millet et al., 2006), and we use the observed relationship between OA and HCHO to evaluate the GEOS-Chem isoprene SOA yields. The SEAC^{4}RS aircraft payload included measurements of OA

ACPD
15, 32005–32047, 2015

from an Aerodyne Aerosol Mass Spectrometer (HR-ToF-AMS; DeCarlo et al., 2006; Canagaratna et al., 2007) concurrent with HCHO from a laser-induced fluorescence instrument (ISAF; Cazorla et al., 2015). Column HCHO was also measured during SEAC^{4}RS from the OMI satellite instrument (Abad et al., 2015; Zhu et al., 2015), providing a proxy for isoprene emission (Palmer et al., 2003, 2006).

Figure 3 (left) shows the observed and simulated relationships between OA and HCHO mixing ratios in the boundary layer. There is a strong correlation in the observations and in the model ($R = 0.79$ and $R = 0.82$, respectively). OA simulated with our aqueous-phase isoprene SOA mechanism reproduces the observed slope ($2.8 \pm 0.3\,\mu g\,s\,m^{-3}\,ppbv^{-1}$, vs. $3.0 \pm 0.4\,\mu g\,s\,m^{-3}\,ppbv^{-1}$ in the observations). Similarly strong correlations and consistency between model and observations are found with column HCHO measured from OMI (Fig. 3, right).

Also shown in Fig. 3 is a sensitivity simulation with the default GEOS-Chem mechanism based on reversible partitioning with pre-existing organic aerosol (Pye et al., 2010) and producing a 1.1 % mean isoprene SOA yield, as compared to 3.3 % in our simulation with the aqueous-phase mechanism. That sensitivity simulation shows the same OA-HCHO correlation ($R = 0.82$) but underestimates the slope ($2.0 \pm 0.3\,\mu g\,s\,m^{-3}\,ppbv^{-1}$). The factor of 3 increase in our isoprene SOA yield does not induce an equivalent response in the slope, as isoprene contributes only ~ 40 % of OA in the Southeast US. But the slope is sensitive to the isoprene SOA yield, and the good agreement between our simulation and observations supports our estimate of a mean 3.3 % yield for the Southeast US.

Figure 3 shows an offset between the model and observations illustrated by the regression lines. We overestimate HCHO by 0.4 ppbv on average because we did not apply the 15 % downward correction to MEGAN v2.1 isoprene emissions (Zhu et al., 2015). We also underestimate total OA measured by the AMS in the boundary layer by $1.1\,\mu g\,s\,m^{-3}$ (mean AMS OA is $5.8 \pm 4.3\,\mu g\,s\,m^{-3}$; model OA is $4.7 \pm 4.4\,\mu g\,s\,m^{-3}$). The bias can be explained by our omission of anthropogenic and open fire SOA, found by Kim et al. (2015) to account on average for 18 % of OA in SEAC^{4}RS.

ACPD
15, 32005–32047, 2015

Figure 4 shows time series of the isoprene SOA components IEPOX SOA and C_5-LVOC SOA at Centreville, Alabama during SOAS. AMS observations from Hu et al. (2015) and Krechmer et al. (2015) are compared to model values. IEPOX SOA and C_5-LVOC SOA are on average 17 and 2 % of total AMS OA, respectively (Hu et al., 2015; Krechmer et al., 2015). The model reproduces the observations without bias, supporting the conclusion that IEPOX is the dominant contributor to isoprene SOA in the Southeast US (Fig. 2). Low values on 2–7 July, both in the observations and the model, are due to low temperatures suppressing isoprene emission.

Figure 5 shows the relationships of daily mean IEPOX SOA and sulfate concentrations at Centreville and in the SEAC^{4}RS boundary layer. The same factor analysis method was used to derive IEPOX SOA in SEAC^{4}RS as in SOAS, however the uncertainty is larger for the aircraft observations due to the much wider range of conditions encountered. There is a strong correlation between IEPOX SOA and sulfate, both in observations and the model, with similar slopes. Correlation between IEPOX SOA and sulfate has similarly been observed at numerous Southeast US monitoring sites (Budisulistiorini et al., 2013, 2015; Xu et al., 2015; Hu et al., 2015). Xu et al. (2015) concluded that IEPOX SOA must form by acid-catalyzed nucleophilic addition of sulfate (sulfate channels in Eq. 2) leading to organosulfates. However, we find in our model that the H^+-catalyzed channel ($k_{H^+}[H^+]$ term in Eq. 2) contributes on average 90 % of IEPOX SOA formation, and that sulfate channels play only a minor role. Thus the correlation of IEPOX SOA and sulfate is not an indication of organosulfate formation but rather reflects the correlation of sulfate with aqueous aerosol volume and acidity. Liao et al. (2015) similarly observed that aerosol acidity and aerosol volume, rather than aerosol sulfate, modulate formation of IEPOX organosulfates in the Southeast US. Measurements from the PALMS laser mass spectrometer during SEAC^{4}RS (Liao et al., 2015) show a mean IEPOX organosulfate concentration of 0.13 $\mu g\,s\,m^{-3}$, amounting to at most 9 % of total IEPOX SOA. The organosulfate should be a marker of the sulfate channels because its hydrolysis is negligibly slow (Hu et al., 2011).

ACPD
15, 32005–32047, 2015

Formation of IEPOX SOA is nearly linear with k_{het} in Eq. (3) as aqueous aerosol is only a minor sink for IEPOX. IEPOX γ is sufficiently small (Table 2) that gas-phase diffusion and mass accommodation are not limiting processes. k_{aq} in Eq. (2) is dominated by the $k_{H^+}[H^+]$ term as discussed above. It follows from combination of Eq. (1), (2), and (3) that IEPOX SOA formation is proportional to $V[H^+]$, where V is the volume concentration of aqueous aerosol. Increasing sulfate increases both V and $[H^+]$, explaining the correlation between IEPOX SOA and sulfate.

Correlation between IEPOX SOA and sulfate is also apparent in the spatial distribution of IEPOX SOA, as observed by the SEAC^{4}RS aircraft below 2 km and simulated by GEOS-Chem along the aircraft flight tracks (Fig. 6). The correlation between simulated and observed IEPOX SOA in Fig. 6 is $R = 0.70$. Average (mean) IEPOX SOA is $1.4 \pm 1.4\,\mu g\,s\,m^{-3}$ in the observations and $1.3 \pm 1.2\,\mu g\,s\,m^{-3}$ in the model. The correlation between IEPOX SOA and sulfate is 0.66 in the observations and 0.77 in the model. IEPOX SOA concentrations are highest in the industrial Midwest and Kentucky, and in Louisiana-Mississippi, coincident with the highest sulfate concentrations sampled on the flights. We also see in Fig. 6 frequent observations of very low IEPOX SOA (less than $0.4\,\mu g\,s\,m^{-3}$) that are well captured by the model. These are associated with very low sulfate (less than $1\,\mu g\,s\,m^{-3}$) leading to high pH and low aerosol volume concentration that have a compounding effect on suppressing IEPOX SOA formation.

The mean IEPOX SOA concentration simulated by the model for the SEAC^{4}RS period (background contours in Fig. 6) is far more uniform than IEPOX SOA simulated along the flight tracks, illustrating the importance of day-to-day variations in sulfate in driving IEPOX SOA variability. IEPOX SOA contributed on average 24 % of total OA in the SEAC^{4}RS observations, 28 % in GEOS-Chem sampled along the flight tracks, and as a regional mean. With IEPOX SOA accounting for 58 % of isoprene SOA in the model (Fig. 2), this amounts to a 41–48 % contribution of isoprene to total OA. Kim et al. (2015) previously estimated a 40 % contribution of isoprene to total OA.

ACPD
15, 32005–32047, 2015

5 Effect of anthropogenic emission reductions

The EPA projects that US anthropogenic emissions of NO_x and SO_2 will decrease respectively by 34 and 48 % from 2013 to 2025 (EPA, 2014). We conducted a GEOS-Chem sensitivity simulation to examine the effect of these changes on isoprene SOA, assuming no other changes and further assuming that the emission decreases are uniform across the US.

Figure 7 shows the individual and combined effects of NO_x and SO_2 emission reductions on the branching pathways for isoprene oxidation, sulfate mass concentration, aerosol pH, and isoprene SOA in the Southeast US boundary layer in summer. Reducing NO_x emission by 34 % decreases the mean NO concentration by only 23 %, in part because decreasing OH increases the NO_x lifetime and in part because decreasing ozone increases the NO/NO_2 ratio. There is no change in HO_2. We find a 10 % decrease in the high-NO_x pathway and a 6 % increase in the low-NO_x pathway involving $ISOPO_2 + HO_2$. Aerosol sulfate decreases by 2 % and there is no change in $[H^+]$. The net effect is a 7 % increase in isoprene SOA, as the major individual components IEPOX SOA and glyoxal SOA increase by 17 % and decrease by 8 %, respectively.

A 48 % decrease in SO_2 emissions drives a 36 % reduction in sulfate mass concentration, leading to a decline in aerosol volume (31 %) that reduces uptake of all isoprene SOA precursors. The decrease in aerosol $[H^+]$ (26 %) further reduces IEPOX uptake. Isoprene SOA mass concentration decreases by 35 % as IEPOX SOA and glyoxal SOA decrease by 45 and 26 %, respectively. Pye et al. (2013) included uptake of IEPOX to aqueous aerosols in a regional chemical transport model and similarly found that SO_2 emissions are more effective than NO_x emissions at reducing IEPOX SOA in the Southeast US. Remarkably, we find that reducing SO_2 emissions decreases sulfate and isoprene SOA with similar effectiveness (Fig. 7). With sulfate contributing ~ 30 % of present-day $PM_{2.5}$ in the Southeast US and isoprene SOA contributing ~ 25 % (Kim et al., 2015), this represents a factor of 2 co-benefit on $PM_{2.5}$ from reducing SO_2 emissions.

ACPD
15, 32005–32047, 2015

Summertime OA and sulfate concentrations in the Southeast declined from 2003 to 2013 at rates of 3.9 % a^{-1} and 7.4 % a^{-1}, respectively, while wintertime OA showed no significant decrease (Kim et al., 2015). With isoprene accounting for 40 % of OA in summer (Kim et al., 2015), and assuming no trend in other OA components on the basis of the wintertime data, we would infer a rate of isoprene SOA decrease of 9.8 % a^{-1}. The observed trends thus seem to support a similar relative rate of decrease of sulfate and isoprene SOA over the past decade.

6 Conclusions

Standard mechanisms for formation of isoprene secondary organic aerosol (SOA) in chemical transport models assume reversible partitioning of isoprene oxidation products to pre-existing dry OA. This may be appropriate for dry conditions in experimental chambers but not for typical atmospheric conditions where the aerosol is mostly aqueous. Here we developed an aqueous-phase reactive uptake mechanism coupled to a detailed gas-phase isoprene chemistry mechanism to describe the irreversible uptake of water-soluble isoprene oxidation products to aqueous aerosol. We applied this mechanism in the GEOS-Chem chemical transport model to simulate surface (SOAS) and aircraft (SEAC^{4}RS) observations over the Southeast US in summer 2013.

Our mechanism includes different channels for isoprene SOA formation by the high-NO_x pathway, when the isoprene peroxy radicals ($ISOPO_2$) react with NO, and in the low-NO_x pathway where they react mostly with HO_2. The main SOA precursors are found to be isoprene epoxide (IEPOX) in the low-NO_x pathway and glyoxal in the high- and low-NO_x pathways. Both of these precursors have dominant gas-phase photochemical sinks, and so their uptake by aqueous aerosol is nearly proportional to the reactive uptake coefficient γ and to the aqueous aerosol mass concentration. The γ for IEPOX is mostly determined by the rate of H^+-catalyzed ring opening in the aqueous phase.

ACPD
15, 32005–32047, 2015

Application of our mechanism to the Southeast US indicates a mean isoprene SOA yield of 3.3 % on a mass basis. By contrast, a conventional mechanism based on reversible uptake of semivolatile isoprene oxidation products yields only 1.1 %. Simulation of the observed relationship of OA with formaldehyde (HCHO) provides support for our higher yield. We find that the low-NO_x pathway is 5 times more efficient than the high-NO_x pathway for isoprene SOA production. Under Southeast US conditions, IEPOX and glyoxal account respectively for 58 and 28 % of isoprene SOA.

Our model simulates well the observations and variability of IEPOX SOA at the surface and from aircraft. The observations show a strong correlation with sulfate that we reproduce in the model. This correlation was previously attributed to acid-catalyzed nucleophilic addition of sulfate as mechanism for IEPOX SOA formation but we find in the model that this pathway is minor. We find instead that the correlation of IEPOX SOA with sulfate is due to the effect of sulfate on aerosol pH and volume concentration, increasing IEPOX uptake by the H^+-catalyzed ring-opening mechanism. Low concentrations of sulfate are associated with very low IEPOX SOA, both in the observations and the model, and we attribute this to the compounding effects of low sulfate on aerosol [H^+] and on aerosol volume.

The US EPA has projected that US NO_x and SO_2 emissions will decrease by 34 and 48 % respectively from 2013 to 2025. We find in our model that the NO_x reduction will increase isoprene SOA by 7 %, reflecting greater importance of the low-NO_x pathway. The SO_2 reduction will decrease isoprene SOA by 35 %, due to decreases in both aerosol [H^+] and volume concentration. The combined effect of these two changes is to decrease isoprene SOA by 32 %, corresponding to a decrease in the isoprene SOA mass yield from 3.3 to 2.3 %. Decreasing SO_2 emissions by 48 % has similar relative effects on sulfate (36 %) and isoprene SOA (35 %). Considering that sulfate presently accounts for about 30 % of $PM_{2.5}$ in the Southeast US in summer, while isoprene SOA contributes 25 %, we conclude that decreasing isoprene SOA represents a factor of 2 co-benefit when reducing SO_2 emissions.

ACPD
15, 32005–32047, 2015

Acknowledgements. We are grateful to the entire NASA SEAC^{4}RS team for their help in the field, in particular Paul Wennberg, John Crounse, Jason St. Clair, and Alex Teng for their CIT-CIMS measurements. Thanks also to Jesse Kroll for assisting in the interpretation of chamber study results. This work was funded by the NASA Tropospheric Chemistry Program, the NASA Air Quality Applied Science Team, and a South African National Research Foundation Fellowship and Schlumberger Faculty for the Future Fellowship to EAM. WH, JEK, PCJ, DAD, and JLJ were supported by NASA NNX12AC03G/NNX15AT96G and NSF AGS-1243354. JEK was supported by EPA STAR (FP-91770901-0) and CIRES Fellowships. JAF acknowledges support from a University of Wollongong Vice Chancellor's Postdoctoral Fellowship. HCHO observations were acquired with support from NASA ROSES SEAC^{4}RS grant NNH10ZDA001N. Although this document has been reviewed by US EPA and approved for publication, it does not necessarily reflect US EPA's policies or views.

References

Anttila, T., Kiendler-Scharr, A., Tillmann, R., and Mentel, T. F.: On the reactive uptake of gaseous compounds by organic-coated aqueous aerosols: theoretical analysis and application to the heterogeneous hydrolysis of N_2O_5, J. Phys. Chem. A, 110, 10435–10443, doi:10.1021/jp062403c, 2006.

Attwood, A. R., Washenfelder, R. A., Brock, C. A., Hu, W., Baumann, K., Campuzano-Jost, P., Day, D. A., Edgerton, E. S., Murphy, D. M., Palm, B. B., McComiskey, A., Wagner, N. L., de Sá, S. S., Ortega, A., Martin, S. T., Jimenez, J. L., and Brown, S. S.: Trends in sulfate and organic aerosol mass in the Southeast US: impact on aerosol optical depth and radiative forcing, Geophys. Res. Lett., 41, 7701–7709, doi:10.1002/2014gl061669, 2014.

Bates, K. H., Crounse, J. D., St. Clair, J. M., Bennett, N. B., Nguyen, T. B., Seinfeld, J. H., Stoltz, B. M., and Wennberg, P. O.: Gas phase production and loss of isoprene epoxydiols, J. Phys. Chem. A, 118, 1237–1246, doi:10.1021/jp4107958, 2014.

Brégonzio-Rozier, L., Giorio, C., Siekmann, F., Pangui, E., Morales, S. B., Temime-Roussel, B., Gratien, A., Michoud, V., Cazaunau, M., DeWitt, H. L., Tapparo, A., Monod, A., and Doussin, J.-F.: Secondary Organic Aerosol formation from isoprene photooxidation during cloud condensation–evaporation cycles, Atmos. Chem. Phys. Discuss., 15, 20561–20596, doi:10.5194/acpd-15-20561-2015, 2015.

ACPD
15, 32005–32047, 2015

Brown, S. S., deGouw, J. A., Warneke, C., Ryerson, T. B., Dubé, W. P., Atlas, E., Weber, R. J., Peltier, R. E., Neuman, J. A., Roberts, J. M., Swanson, A., Flocke, F., McKeen, S. A., Brioude, J., Sommariva, R., Trainer, M., Fehsenfeld, F. C., and Ravishankara, A. R.: Nocturnal isoprene oxidation over the Northeast United States in summer and its impact on reactive nitrogen partitioning and secondary organic aerosol, Atmos. Chem. Phys., 9, 3027–3042, doi:10.5194/acp-9-3027-2009, 2009.

Budisulistiorini, S. H., Canagaratna, M. R., Croteau, P. L., Marth, W. J., Baumann, K., Edgerton, E. S., Shaw, S. L., Knipping, E. M., Worsnop, D. R., Jayne, J. T., Gold, A., and Surratt, J. D.: Real-time continuous characterization of secondary organic aerosol derived from isoprene epoxydiols in downtown Atlanta, Georgia, using the Aerodyne aerosol chemical speciation monitor, Environ. Sci. Technol., 47, 5686–5694, doi:10.1021/es400023n, 2013.

Budisulistiorini, S. H., Li, X., Bairai, S. T., Renfro, J., Liu, Y., Liu, Y. J., McKinney, K. A., Martin, S. T., McNeill, V. F., Pye, H. O. T., Nenes, A., Neff, M. E., Stone, E. A., Mueller, S., Knote, C., Shaw, S. L., Zhang, Z., Gold, A., and Surratt, J. D.: Examining the effects of anthropogenic emissions on isoprene-derived secondary organic aerosol formation during the 2013 Southern Oxidant and Aerosol Study (SOAS) at the Look Rock, Tennessee ground site, Atmos. Chem. Phys., 15, 8871–8888, doi:10.5194/acp-15-8871-2015, 2015.

Buxton, G. V., Malone, T. N., and Salmon, G. A.: Oxidation of glyoxal initiated by $^{\bullet}$OH in oxygenated aqueous solution, J. Chem. Soc. Faraday T., 93, 2889–2891, doi:10.1039/A701468f, 1997.

Canagaratna, M. R., Jayne, J. T., Jimenez, J. L., Allan, J. D., Alfarra, M. R, Zhang, Q., Onasch, T. B., Drewnick, F., Coe, H., Middlebrook, A., Delia, A., Williams, L. R., Trimborn, A. M., Northway, M. J., DeCarlo, P. F., Kolb, C. E., Davidovits, P., Worsnop, D. R.: Chemical and microphysical characterization of ambient aerosols with the Aerodyne Aerosol Mass Spectrometer, Mass Spectrom. Rev., 26, 185–222, doi:10.1002/mas.20115, 2007.

Carlton, A. G. and Turpin, B. J.: Particle partitioning potential of organic compounds is highest in the Eastern US and driven by anthropogenic water, Atmos. Chem. Phys., 13, 10203–10214, doi:10.5194/acp-13-10203-2013, 2013.

Carlton, A. G., Wiedinmyer, C., and Kroll, J. H.: A review of Secondary Organic Aerosol (SOA) formation from isoprene, Atmos. Chem. Phys., 9, 4987–5005, doi:10.5194/acp-9-4987-2009, 2009.

Cazorla, M., Wolfe, G. M., Bailey, S. A., Swanson, A. K., Arkinson, H. L., and Hanisco, T. F.: A new airborne laser-induced fluorescence instrument for in situ detection of formalde-

ACPD
15, 32005–32047, 2015

hyde throughout the troposphere and lower stratosphere, Atmos. Meas. Tech., 8, 541–552, doi:10.5194/amt-8-541-2015, 2015.
Chan, A. W. H., Chan, M. N., Surratt, J. D., Chhabra, P. S., Loza, C. L., Crounse, J. D., Yee, L. D., Flagan, R. C., Wennberg, P. O., and Seinfeld, J. H.: Role of aldehyde chemistry and NO_x concentrations in secondary organic aerosol formation, Atmos. Chem. Phys., 10, 7169–7188, doi:10.5194/acp-10-7169-2010, 2010.
Cole-Filipiak, N. C., O'Connor, A. E., and Elrod, M. J.: Kinetics of the hydrolysis of atmospherically relevant isoprene-derived hydroxy epoxides, Environ. Sci. Technol., 44, 6718–6723, doi:10.1021/es1019228, 2010.
Darer, A. I., Cole-Filipiak, N. C., O'Connor, A. E., and Elrod, M. J.: Formation and stability of atmospherically relevant isoprene-derived organosulfates and organonitrates, Environ. Sci. Technol., 45, 1895–1902, doi:10.1021/es103797z, 2011.
DeCarlo, P. F., Kimmel, J. R. Trimborn, A., Northway, M. J., Jayne, J. T., Aiken, A. C., Gonin, M., Fuhrer, K., Horvath, T., Docherty, K. S., Worsnop, D. R., and Jimenez, J. L.: Field-deployable, High-Resolution, Time-of-Flight Aerosol Mass Spectrometer, Anal. Chem., 78, 8281–8289, doi:10.1021/ac061249n, 2006.
Dommen, J., Metzger, A., Duplissy, J., Kalberer, M., Alfarra, M. R., Gascho, A., Weingartner, E., Prévôt, A. S. H., Verheggen, B., and Baltensperger, U.: Laboratory observation of oligomers in the aerosol from isoprene/NO_x photooxidation, Geophys. Res. Lett., 33, L13805, doi:10.1029/2006gl026523, 2006.
Donahue, N. M., Robinson, A. L., Stanier, C. O., and Pandis, S. N.: Coupled partitioning, dilution, and chemical aging of semivolatile organics, Environ. Sci. Technol., 40, 2635–2643, doi:10.1021/es052297c, 2006.
Drury, E., Jacob, D. J., Spurr, R. J. D., Wang, J., Shinozuka, Y., Anderson, B. E., Clarke, A. D., Dibb, J., McNaughton, C., and Weber, R.: Synthesis of satellite (MODIS), aircraft (ICARTT), and surface (IMPROVE, EPA-AQS, AERONET) aerosol observations over eastern North America to improve MODIS aerosol retrievals and constrain surface aerosol concentrations and sources, J. Geophys. Res., 115, D14204, doi:10.1029/2009jd012629, 2010.
Eddingsaas, N. C., VanderVelde, D. G., and Wennberg, P. O.: Kinetics and products of the acid-catalyzed ring-opening of atmospherically relevant butyl epoxy alcohols, J. Phys. Chem. A, 114, 8106–8113, doi:10.1021/jp103907c, 2010.
Edney, E. O., Kleindienst, T. E., Jaoui, M., Lewandowski, M., Offenberg, J. H., Wang, W., and Claeys, M.: Formation of 2-methyl tetrols and 2-methylglyceric acid in secondary organic

ACPD
15, 32005–32047, 2015

aerosol from laboratory irradiated isoprene/NO_x/SO_2/air mixtures and their detection in ambient $PM_{2.5}$ samples collected in the eastern United States, Atmos. Environ., 39, 5281–5289, doi:10.1016/j.atmosenv.2005.05.031, 2005.

EPA: U.S. Environmental Protection Agency, Technical Support Document (TSD): preparation of Emissions Inventories for the Version 6.1, 2011 Emissions Modeling Platform, available at: http://www.epa.gov/ttn/chief/emch/2011v6/2011v6.1_2018_2025_base_EmisMod_TSD_nov2014_v6.pdf (last access: 15 July 2015), 2014.

Ervens, B., Gligorovski, S., and Herrmann, H.: Temperature-dependent rate constants for hydroxyl radical reactions with organic compounds in aqueous solutions, Phys. Chem. Chem. Phys., 5, 1811–1824, doi:10.1039/b300072a, 2003.

Ervens, B., Turpin, B. J., and Weber, R. J.: Secondary organic aerosol formation in cloud droplets and aqueous particles (aqSOA): a review of laboratory, field and model studies, Atmos. Chem. Phys., 11, 11069–11102, doi:10.5194/acp-11-11069-2011, 2011.

Fisher, J. A., Jacob, D., Travis, K., Cohen, R., Fried, A., Hanisco, T., Mao, J., Wennberg, P., Crounse, J., St. Clair, J., Teng, A., Wisthaler, A., Mikoviny, T., Jimenez, J., Campuzano-Jost, P., Kim., P., Marais, E., Paulot, F., Yu, K., Zhu, L., Yantosca, R., and Sulprizio, M.: Organic nitrate chemistry and its implications for nitrogen budgets in the Southeast US constrained by aircraft (SEAC^{4}RS) and ground-based (SOAS) observations, in preparation, 2015.

Fountoukis, C. and Nenes, A.: ISORROPIA II: a computationally efficient thermodynamic equilibrium model for K^+–Ca^{2+}–Mg^{2+}–NH_4^+–Na^+–SO_4^{2-}–NO_3^-–Cl^-–H_2O aerosols, Atmos. Chem. Phys., 7, 4639–4659, doi:10.5194/acp-7-4639-2007, 2007.

Fu, T.-M., Jacob, D. J., Wittrock, F., Burrows, J. P., Vrekoussis, M., and Henze, D. K.: Global budgets of atmospheric glyoxal and methylglyoxal, and implications for formation of secondary organic aerosols, J. Geophys. Res., 113, D15303, doi:10.1029/2007jd009505, 2008.

Gaston, C. J., Riedel, T. P., Zhang, Z., Gold, A., Surratt, J. D., and Thornton, J. A.: Reactive uptake of an isoprene-derived epoxydiol to submicron aerosol particles, Environ. Sci. Technol., 48, 11178–11186, doi:10.1021/es5034266, 2014.

González Abad, G., Liu, X., Chance, K., Wang, H., Kurosu, T. P., and Suleiman, R.: Updated Smithsonian Astrophysical Observatory Ozone Monitoring Instrument (SAO OMI) formaldehyde retrieval, Atmos. Meas. Tech., 8, 19–32, doi:10.5194/amt-8-19-2015, 2015.

Guenther, A., Karl, T., Harley, P., Wiedinmyer, C., Palmer, P. I., and Geron, C.: Estimates of global terrestrial isoprene emissions using MEGAN (Model of Emissions of Gases and

ACPD
15, 32005–32047, 2015

Aerosols from Nature), Atmos. Chem. Phys., 6, 3181–3210, doi:10.5194/acp-6-3181-2006, 2006.
Guenther, A. B., Jiang, X., Heald, C. L., Sakulyanontvittaya, T., Duhl, T., Emmons, L. K., and Wang, X.: The Model of Emissions of Gases and Aerosols from Nature version 2.1 (MEGAN2.1): an extended and updated framework for modeling biogenic emissions, Geosci. Model Dev., 5, 1471–1492, doi:10.5194/gmd-5-1471-2012, 2012.
Guo, H., Xu, L., Bougiatioti, A., Cerully, K. M., Capps, S. L., Hite Jr., J. R., Carlton, A. G., Lee, S.-H., Bergin, M. H., Ng, N. L., Nenes, A., and Weber, R. J.: Fine-particle water and pH in the southeastern United States, Atmos. Chem. Phys., 15, 5211–5228, doi:10.5194/acp-15-5211-2015, 2015.
Hallquist, M., Wenger, J. C., Baltensperger, U., Rudich, Y., Simpson, D., Claeys, M., Dommen, J., Donahue, N. M., George, C., Goldstein, A. H., Hamilton, J. F., Herrmann, H., Hoffmann, T., Iinuma, Y., Jang, M., Jenkin, M. E., Jimenez, J. L., Kiendler-Scharr, A., Maenhaut, W., McFiggans, G., Mentel, Th. F., Monod, A., Prévôt, A. S. H., Seinfeld, J. H., Surratt, J. D., Szmigielski, R., and Wildt, J.: The formation, properties and impact of secondary organic aerosol: current and emerging issues, Atmos. Chem. Phys., 9, 5155–5236, doi:10.5194/acp-9-5155-2009, 2009.
Hess, M., Koepke, P., and Schult, I.: Optical properties of aerosols and clouds: the software package OPAC, B. Am. Meteorol. Soc., 79, 831–844, 1998.
Hodzic, A. and Jimenez, J. L.: Modeling anthropogenically controlled secondary organic aerosols in a megacity: a simplified framework for global and climate models, Geosci. Model Dev., 4, 901–917, doi:10.5194/gmd-4-901-2011, 2011.
Hu, K. S., Darer, A. I., and Elrod, M. J.: Thermodynamics and kinetics of the hydrolysis of atmospherically relevant organonitrates and organosulfates, Atmos. Chem. Phys., 11, 8307–8320, doi:10.5194/acp-11-8307-2011, 2011.
Hu, W. W., Campuzano-Jost, P., Palm, B. B., Day, D. A., Ortega, A. M., Hayes, P. L., Krechmer, J. E., Chen, Q., Kuwata, M., Liu, Y. J., de Sá, S. S., McKinney, K., Martin, S. T., Hu, M., Budisulistiorini, S. H., Riva, M., Surratt, J. D., St. Clair, J. M., Isaacman-Van Wertz, G., Yee, L. D., Goldstein, A. H., Carbone, S., Brito, J., Artaxo, P., de Gouw, J. A., Koss, A., Wisthaler, A., Mikoviny, T., Karl, T., Kaser, L., Jud, W., Hansel, A., Docherty, K. S., Alexander, M. L., Robinson, N. H., Coe, H., Allan, J. D., Canagaratna, M. R., Paulot, F., and Jimenez, J. L.: Characterization of a real-time tracer for isoprene epoxydiols-derived secondary or-

ACPD
15, 32005–32047, 2015

ganic aerosol (IEPOX-SOA) from aerosol mass spectrometer measurements, Atmos. Chem. Phys., 15, 11807–11833, doi:10.5194/acp-15-11807-2015, 2015.
Jacob, D. J.: Heterogeneous chemistry and tropospheric ozone, Atmos. Environ., 34, 2131–2159, doi:10.1016/s1352-2310(99)00462-8, 2000.
Jacobs, M. I., Darer, A. I., and Elrod, M. J.: Rate constants and products of the OH reaction with isoprene-derived epoxides, Environ. Sci. Technol., 47, 12868–12876, doi:10.1021/es403340g, 2013.
Jacobs, M. I., Burke, W. J., and Elrod, M. J.: Kinetics of the reactions of isoprene-derived hydroxynitrates: gas phase epoxide formation and solution phase hydrolysis, Atmos. Chem. Phys., 14, 8933–8946, doi:10.5194/acp-14-8933-2014, 2014.
Kim, P. S., Jacob, D. J., Fisher, J. A., Travis, K., Yu, K., Zhu, L., Yantosca, R. M., Sulprizio, M. P., Jimenez, J. L., Campuzano-Jost, P., Froyd, K. D., Liao, J., Hair, J. W., Fenn, M. A., Butler, C. F., Wagner, N. L., Gordon, T. D., Welti, A., Wennberg, P. O., Crounse, J. D., St. Clair, J. M., Teng, A. P., Millet, D. B., Schwarz, J. P., Markovic, M. Z., and Perring, A. E.: Sources, seasonality, and trends of southeast US aerosol: an integrated analysis of surface, aircraft, and satellite observations with the GEOS-Chem chemical transport model, Atmos. Chem. Phys., 15, 10411–10433, doi:10.5194/acpd-15-10411-2015, 2015.
King, S. M., Rosenoern, T., Shilling, J. E., Chen, Q., Wang, Z., Biskos, G., McKinney, K. A., Pöschl, U., and Martin, S. T.: Cloud droplet activation of mixed organic-sulfate particles produced by the photooxidation of isoprene, Atmos. Chem. Phys., 10, 3953–3964, doi:10.5194/acp-10-3953-2010, 2010.
Kleindienst, T. E., Edney, E. O., Lewandowski, M., Offenberg, J. H., and Jaoui, M.: Secondary organic carbon and aerosol yields from the irradiations of isoprene and α-pinene in the presence of NO_x and SO_2, Environ. Sci. Technol., 40, 3807–3812, doi:10.1021/es052446r, 2006.
Kleindienst, T. E., Lewandowski, M., Offenberg, J. H., Jaoui, M., and Edney, E. O.: Ozone-isoprene reaction: re-examination of the formation of secondary organic aerosol, Geophys. Res. Lett., 34, L01805, doi:10.1029/2006gl027485, 2007.
Kleindienst, T. E., Lewandowski, M., Offenberg, J. H., Jaoui, M., and Edney, E. O.: The formation of secondary organic aerosol from the isoprene + OH reaction in the absence of NO_x, Atmos. Chem. Phys., 9, 6541–6558, doi:10.5194/acp-9-6541-2009, 2009.
Knote, C., Hodzic, A., Jimenez, J. L., Volkamer, R., Orlando, J. J., Baidar, S., Brioude, J., Fast, J., Gentner, D. R., Goldstein, A. H., Hayes, P. L., Knighton, W. B., Oetjen, H., Setyan, A., Stark, H., Thalman, R., Tyndall, G., Washenfelder, R., Waxman, E., and Zhang, Q.: Simula-

ACPD
15, 32005–32047, 2015

tion of semi-explicit mechanisms of SOA formation from glyoxal in aerosol in a 3-D model, Atmos. Chem. Phys., 14, 6213–6239, doi:10.5194/acp-14-6213-2014, 2014.

Koepke, P., Hess, M., Schult, I., and Shettle, E. P.: Global aerosol data set, report, Max-Planck Inst. für Meteorol., Hamburg, Germany, 1997.

Krechmer, J. E., Coggon, M. M., Massoli, P., Nguyen, T. B., Crounse, J. D., Hu, W., Day, D. A., Tyndall, G. S., Henze, D. K., Rivera-Rios, J. C., Nowak, J. B., Kimmel, J. R., Mauldin, III, R. L., Stark, H., Jayne, J. T., Sipilä, M., Junninen, H., St. Clair, J. M., Zhang, X., Feiner, P. A., Zhang, L., Miller, D. O., Brune, W. H., Keutsch, F. N., Wennberg, P. O., Seinfeld, J. H., Worsnop, D. R., Jimenez, J. L., and Canagaratna, M. R.: Formation of low volatility organic compounds and secondary organic aerosol from isoprene hydroxyhydroperoxide low-NO oxidation, Environ. Sci. Technol., 49, 10330–10339, doi:10.1021/acs.est.5b02031, 2015.

Kroll, J. H., Ng, N. L., Murphy, S. M., Flagan, R. C., and Seinfeld, J. H.: Secondary organic aerosol formation from isoprene photooxidation under high-NO_x conditions, Geophys. Res. Lett., 32, L18808, doi:10.1029/2005gl023637, 2005.

Kroll, J. H., Ng, N. L., Murphy, S. M., Flagan, R. C., and Seinfeld, J. H.: Secondary organic aerosol formation from isoprene photooxidation, Environ. Sci. Technol., 40, 1869–1877, doi:10.1021/es0524301, 2006.

Lee, L., Teng, A. P., Wennberg, P. O., Crounse, J. D., and Cohen, R. C.: On rates and mechanisms of OH and O_3 reactions with isoprene-derived hydroxy nitrates, J. Phys. Chem. A, 118, 1622–1637, doi:10.1021/jp4107603, 2014.

Lewandowski, M., Jaoui, M., Offenberg, J. H., Krug, J. D., and Kleindienst, T. E.: Atmospheric oxidation of isoprene and 1,3-butadiene: influence of aerosol acidity and relative humidity on secondary organic aerosol, Atmos. Chem. Phys., 15, 3773–3783, doi:10.5194/acp-15-3773-2015, 2015.

Liao, J., Froyd, K. D., Murphy, D. M., Keutsch, F. N., Yu, G., Wennberg, P. O., St. Clair, J. M., Crounse, J. D., Wisthaler, A., Mikoviny, T., Jimenez, J. L., Campuzano-Jost, P., Day, D. A., Hu, W., Ryerson, T. B., Pollack, I. B., Peischl, J., Anderson, B. E., Ziemba, L. D., Blake, D. R., Meinardi, S., and Diskin, G.: Airborne measurements of organosulfates over the continental US, J. Geophys. Res., 120, 2990–3005, doi:10.1002/2014jd022378, 2015.

Liggio, J., Li, S.-M., and McLaren, R.: Reactive uptake of glyoxal by particulate matter, J. Geophys. Res., 110, D10304, doi:10.1029/2004jd005113, 2005.

Lin, Y.-H., Zhang, H., Pye, H. O. T., Zhang, Z. F., Marth, W. J., Park, S., Arashiro, M., Cui, T., Budisulistiorini, S. H., Sexton, K. G., Vizuete, W., Xie, Y., Luecken, D. J., Piletic, I. R., Ed-

ACPD
15, 32005–32047, 2015

ney, E. O., Bartolotti, L. J., Gold, A., and Surratt, J. D.: Epoxide as a precursor to secondary organic aerosol formation from isoprene photooxidation in the presence of nitrogen oxides, P. Natl. Acad. Sci. USA, 110, 6718–6723, doi:10.1073/pnas.1221150110, 2013.

Liu, Y. J., Herdlinger-Blatt, I., McKinney, K. A., and Martin, S. T.: Production of methyl vinyl ketone and methacrolein via the hydroperoxyl pathway of isoprene oxidation, Atmos. Chem. Phys., 13, 5715–5730, doi:10.5194/acp-13-5715-2013, 2013.

Mao, J., Paulot, F., Jacob, D. J., Cohen, R. C., Crounse, J. D., Wennberg, P. O., Keller, C. A., Hudman, R. C., Barkley, M. P., and Horowitz, L. W.: Ozone and organic nitrates over the eastern United States: sensitivity to isoprene chemistry, J. Geophys. Res., 118, 11256–11268, doi:10.1002/jgrd.50817, 2013.

Martin, R. V., Jacob, D. J., Yantosca, R. M., Chin, M., and Ginoux, P.: Global and regional decreases in tropospheric oxidants from photochemical effects of aerosols, J. Geophys. Res., 108, 4097, doi:10.1029/2002jd002622, 2003.

McNeill, V. F., Woo, J. L., Kim, D. D., Schwier, A. N., Wannell, N. J., Sumner, A. J., and Barakat, J. M.: Aqueous-phase secondary organic aerosol and organosulfate formation in atmospheric aerosols: a modeling study, Environ. Sci. Technol., 46, 8075–8081, doi:10.1021/es3002986, 2012.

McNeill, V. F., Sareen, N., and Schwier, A. N.: Surface-active organics in atmospheric aerosols, Top. Curr. Chem., 339, 201–259, doi:10.1007/128_2012_404, 2014.

Millet, D. B., Jacob, D. J., Turquety, S., Hudman, R. C., Wu, S., Fried, A., Walega, J., Heikes, B. G., Blake, D. R., Singh, H. B., Anderson, B. E., and Clarke, A. D.: Formaldehyde distribution over North America: implications for satellite retrievals of formaldehyde columns and isoprene emission, J. Geophys. Res., 111, D24S02, doi:10.1029/2005jd006853, 2006.

Ng, N. L., Kwan, A. J., Surratt, J. D., Chan, A. W. H., Chhabra, P. S., Sorooshian, A., Pye, H. O. T., Crounse, J. D., Wennberg, P. O., Flagan, R. C., and Seinfeld, J. H.: Secondary organic aerosol (SOA) formation from reaction of isoprene with nitrate radicals (NO_3), Atmos. Chem. Phys., 8, 4117–4140, doi:10.5194/acp-8-4117-2008, 2008.

Nguyen, T. B., Coggon, M. M., Bates, K. H., Zhang, X., Schwantes, R. H., Schilling, K. A., Loza, C. L., Flagan, R. C., Wennberg, P. O., and Seinfeld, J. H.: Organic aerosol formation from the reactive uptake of isoprene epoxydiols (IEPOX) onto non-acidified inorganic seeds, Atmos. Chem. Phys., 14, 3497–3510, doi:10.5194/acp-14-3497-2014, 2014.

Nguyen, T. B., Bates, K. H., Crounse, J. D., Schwantes, R. H., Zhang, X., Kjaergaard, H. G., Surratt, J. D., Lin, P., Laskin, A., Seinfeld, J. H., and Wennberg, P. O.: Mechanism of the hydroxyl

ACPD
15, 32005–32047, 2015

radical oxidation of methacryloyl peroxynitrate (MPAN) and its pathway toward secondary organic aerosol formation in the atmosphere, Phys. Chem. Chem. Phys., 17, 17914–17926, doi:10.1039/c5cp02001h, 2015a.

Nguyen, T. B., Crounse, J. D., Teng, A. P., St. Clair, J. M., Paulot, F., Wolfe, G. M., and Wennberg, P. O.: Rapid deposition of oxidized biogenic compounds to a temperate forest, P. Natl. Acad. Sci. USA, 112, E392-E401, doi:10.1073/pnas.1418702112, 2015b.

Nozière, B., Dziedzic, P., and Córdova, A.: Products and kinetics of the liquid-phase reaction of glyoxal catalyzed by ammonium ions (NH_4^+), J. Phys. Chem. A, 113, 231–237, doi:10.1021/jp8078293, 2009.

Odum, J. R., Hoffmann, T., Bowman, F., Collins, D., Flagan, R. C., and Seinfeld, J. H.: Gas/particle partitioning and secondary organic aerosol yields, Environ. Sci. Technol., 30, 2580–2585, doi:10.1021/es950943+, 1996.

Palmer, P. I., Jacob, D. J., Fiore, A. M., Martin, R. V., Chance, K., and Kurosu, T. P.: Mapping isoprene emissions over North America using formaldehyde column observations from space, J. Geophys. Res., 108, 4180, doi:10.1029/2002jd002153, 2003.

Palmer, P. I., Abbot, D. S., Fu, T.-M., Jacob, D. J., Chance, K., Kurosu, T. P., Guenther, A., Wiedinmyer, C., Stanton, J. C., Pilling, M. J., Pressley, S. N., Lamb, B., and Sumner, A. L.: Quantifying the seasonal and interannual variability of North American isoprene emissions using satellite observations of the formaldehyde column, J. Geophys. Res., 111, D12315, doi:10.1029/2005jd006689, 2006.

Paulot, F., Crounse, J. D., Kjaergaard, H. G., Kroll, J. H., Seinfeld, J. H., and Wennberg, P. O.: Isoprene photooxidation: new insights into the production of acids and organic nitrates, Atmos. Chem. Phys., 9, 1479–1501, doi:10.5194/acp-9-1479-2009, 2009a.

Paulot, F., Crounse, J. D., Kjaergaard, H. G., Kürten, A., St. Clair, J. M., Seinfeld, J. H., and Wennberg, P. O.: Unexpected epoxide formation in the gas-phase photooxidation of isoprene, Science, 325, 730–733, doi:10.1126/science.1172910, 2009b.

Peeters, J. and Müller, J.-F.: HO_x radical regeneration in isoprene oxidation via peroxy radical isomerisations. II: Experimental evidence and global impact, Phys. Chem. Chem. Phys., 12, 14227–14235, doi:10.1039/c0cp00811g, 2010.

Peeters, J., Nguyen, T. L., and Vereecken, L.: HO_x radical regeneration in the oxidation of isoprene, Phys. Chem. Chem. Phys., 11, 5935–5939, doi:10.1039/b908511d, 2009.

ACPD
15, 32005–32047, 2015

Piletic, I. R., Edney, E. O., and Bartolotti, L. J.: A computational study of acid catalyzed aerosol reactions of atmospherically relevant epoxides, Phys. Chem. Chem. Phys., 15, 18065–18076, doi:10.1039/c3cp52851k, 2013.

Pye, H. O. T., Chan, A. W. H., Barkley, M. P., and Seinfeld, J. H.: Global modeling of organic aerosol: the importance of reactive nitrogen (NO_x and NO_3), Atmos. Chem. Phys., 10, 11261–11276, doi:10.5194/acp-10-11261-2010, 2010.

Pye, H. O. T., Pinder, R. W., Piletic, I. R., Xie, Y., Capps, S. L., Lin, Y.-H., Surratt, J. D., Zhang, Z., Gold, A., Luecken, D. J., Hutzell, W. T., Jaoui, M., Offenberg, J. H., Kleindienst, T. E., Lewandowski, M., and Edney, E. O.: Epoxide pathways improve model predictions of isoprene markers and reveal key role of acidity in aerosol formation, Environ. Sci. Technol., 47, 11056–11064, doi:10.1021/es402106h, 2013.

Riedel, T. P., Lin, Y.-H., Budisulistiorini, S. H., Gaston, C. J., Thornton, J. A., Zhang, Z. F., Vizuete, W., Gold, A., and Surratt, J. D.: Heterogeneous reactions of isoprene-derived epoxides: reaction probabilities and molar secondary organic aerosol yield estimates, Environ. Sci. Technol. Lett., 2, 38–42, doi:10.1021/ez500406f, 2015.

Rollins, A. W., Kiendler-Scharr, A., Fry, J. L., Brauers, T., Brown, S. S., Dorn, H.-P., Dubé, W. P., Fuchs, H., Mensah, A., Mentel, T. F., Rohrer, F., Tillmann, R., Wegener, R., Wooldridge, P. J., and Cohen, R. C.: Isoprene oxidation by nitrate radical: alkyl nitrate and secondary organic aerosol yields, Atmos. Chem. Phys., 9, 6685–6703, doi:10.5194/acp-9-6685-2009, 2009.

Sato, K., Nakao, S., Clark, C. H., Qi, L., and Cocker III, D. R.: Secondary organic aerosol formation from the photooxidation of isoprene, 1,3-butadiene, and 2,3-dimethyl-1,3-butadiene under high NO_x conditions, Atmos. Chem. Phys., 11, 7301–7317, doi:10.5194/acp-11-7301-2011, 2011.

Saxena, P. and Hildemann, L. M.: Water-soluble organics in atmospheric particles: a critical review of the literature and application of thermodynamics to identify candidate compounds, J. Atmos. Chem., 24, 57–109, doi:10.1007/bf00053823, 1996.

Schwartz, S. E.: Mass-transport considerations pertinent to aqueous-phase reactions of gases in liquid-water clouds, in: Chemistry of Multiphase Atmospheric Systems, Jaechske, W. (Ed.), Springer, Heidelberg, 415–471, 1986.

Scott, C. E., Rap, A., Spracklen, D. V., Forster, P. M., Carslaw, K. S., Mann, G. W., Pringle, K. J., Kivekäs, N., Kulmala, M., Lihavainen, H., and Tunved, P.: The direct and indirect radiative effects of biogenic secondary organic aerosol, Atmos. Chem. Phys., 14, 447–470, doi:10.5194/acp-14-447-2014, 2014.

ACPD
15, 32005–32047, 2015

SEAC^{4}RS Archive, doi:10.5067/Aircraft/SEAC4RS/Aerosol-TraceGas-Cloud.
Song, M., Liu, P. F., Hanna, S. J., Li, Y. J., Martin, S. T., and Bertram, A. K.: Relative humidity-dependent viscosities of isoprene-derived secondary organic material and atmospheric implications for isoprene-dominant forests, Atmos. Chem. Phys., 15, 5145–5159, doi:10.5194/acp-15-5145-2015, 2015.
Stavrakou, T., Peeters, J., and Müller, J.-F.: Improved global modelling of HO_x recycling in isoprene oxidation: evaluation against the GABRIEL and INTEX-A aircraft campaign measurements, Atmos. Chem. Phys., 10, 9863–9878, doi:10.5194/acp-10-9863-2010, 2010.
St. Clair, J. M., Rivera-Rios, J. C., Crounse, J. D., Knap, H. C., Bates, K. H., Teng, A. P., Jørgensen, S., Kjaergaard, H. G., Keutsch, F. N., and Wennberg, P. O.: Kinetics and products of the reaction of the first-generation isoprene hydroperoxide (ISOPOOH) with OH, J. Phys. Chem. A, in press, doi:10.1021/acs.jpca.5b06532, 2015.
Sumner, A. J., Woo, J. L., and McNeill, V. F.: Model Analysis of secondary organic aerosol formation by glyoxal in laboratory studies: the case for photoenhanced chemistry, Environ. Sci. Technol., 48, 11919–11925, doi:10.1021/es502020j, 2014.
Surratt, J. D., Murphy, S. M., Kroll, J. H., Ng, N. L., Hildebrandt, L., Sorooshian, A., Szmigielski, R., Vermeylen, R., Maenhaut, W., Claeys, M., Flagan, R. C., and Seinfeld, J. H.: Chemical composition of secondary organic aerosol formed from the photooxidation of isoprene, J. Phys. Chem. A, 110, 9665–9690, doi:10.1021/jp061734m, 2006.
Surratt, J. D., Kroll, J. H., Kleindienst, T. E., Edney, E. O., Claeys, M., Sorooshian, A., Ng, N. L., Offenberg, J. H., Lewandowski, M., Jaoui, M., Flagan, R. C., and Seinfeld, J. H.: Evidence for organosulfates in secondary organic aerosol, Environ. Sci. Technol., 41, 517–527, doi:10.1021/es062081q, 2007a.
Surratt, J. D., Lewandowski, M., Offenberg, J. H., Jaoui, M., Kleindienst, T. E., Edney, E. O., and Seinfeld, J. H.: Effect of acidity on secondary organic aerosol formation from isoprene, Environ. Sci. Technol., 41, 5363–5369, doi:10.1021/es0704176, 2007b.
Surratt, J. D., Chan, A. W. H., Eddingsaas, N. C., Chan, M., Loza, C. L., Kwan, A. J., Hersey, S. P., Flagan, R. C., Wennberg, P. O., and Seinfeld, J. H.: Reactive intermediates revealed in secondary organic aerosol formation from isoprene, P. Natl. Acad. Sci. USA, 107, 6640–6645, doi:10.1073/pnas.0911114107, 2010.
Tan, Y., Perri, M. J., Seitzinger, S. P., and Turpin, B. J.: Effects of precursor concentration and acidic sulfate in aqueous glyoxal-OH radical oxidation and implications for secondary organic aerosol, Environ. Sci. Technol., 43, 8105–8112, doi:10.1021/es901742f, 2009.

ACPD
15, 32005–32047, 2015

Tan, Y., Carlton, A. G., Seitzinger, S. P., and Turpin, B. J.: SOA from methylglyoxal in clouds and wet aerosols: measurement and prediction of key products, Atmos. Environ., 44, 5218–5226, doi:10.1016/j.atmosenv.2010.08.045, 2010.

Toon, O. B. and the SEAC^{4}RS science team: planning, implementation, and scientific goals of the Studies of Emissions and Atmospheric Composition, Clouds, and Climate Coupling by Regional Surveys (SEAC^{4}RS) field mission, J. Geophys. Res., submitted, 2015.

Travis, K. R., Jacob, D. J., Fisher, J. A., Kim, P. S., Marais, E. A., Zhu, L., Miller, C. C., Wennberg, P. O., Crounse, J., Hanisco, T. A., Ryerson, T., Yu, K., Wolfe, G. M., Thompson, A., Mao, J., Paulot, F., Yantosca, R. M., Sulprizio, M., and Neuman, A.: Implications of rapidly declining NO_x emissions for ozone-NO_x-VOC chemistry in the Southeast United States, in preparation, 2015.

Virtanen, A., Joutsensaari, J., Koop, T., Kannosto, J., Yli-Pirilä, P., Leskinen, J., Mäkelä, J. M., Holopainen, J. K., Pöschl, U., Kulmala, M., Worsnop, D. R., and Laaksonen, A.: An amorphous solid state of biogenic secondary organic aerosol particles, Nature, 467, 824–827, doi:10.1038/nature09455, 2010.

Volkamer, R., Martini, F. S., Molina, L. T., Salcedo, D., Jimenez, J. L., and Molina, M. J.: A missing sink for gas-phase glyoxal in Mexico City: formation of secondary organic aerosol, Geophys. Res. Lett., 34, L19807, doi:10.1029/2007gl030752, 2007.

Volkamer, R., Ziemann, P. J., and Molina, M. J.: Secondary Organic Aerosol Formation from Acetylene (C_2H_2): seed effect on SOA yields due to organic photochemistry in the aerosol aqueous phase, Atmos. Chem. Phys., 9, 1907–1928, doi:10.5194/acp-9-1907-2009, 2009.

Wagner, N. L., Brock, C. A., Angevine, W. M., Beyersdorf, A., Campuzano-Jost, P., Day, D., de Gouw, J. A., Diskin, G. S., Gordon, T. D., Graus, M. G., Holloway, J. S., Huey, G., Jimenez, J. L., Lack, D. A., Liao, J., Liu, X., Markovic, M. Z., Middlebrook, A. M., Mikoviny, T., Peischl, J., Perring, A. E., Richardson, M. S., Ryerson, T. B., Schwarz, J. P., Warneke, C., Welti, A., Wisthaler, A., Ziemba, L. D., and Murphy, D. M.: In situ vertical profiles of aerosol extinction, mass, and composition over the southeast United States during SENEX and SEAC^{4}RS: observations of a modest aerosol enhancement aloft, Atmos. Chem. Phys., 15, 7085–7102, doi:10.5194/acp-15-7085-2015, 2015.

Wang, J., Hoffmann, A. A., Park, R. J., Jacob, D. J., and Martin, S. T.: Global distribution of solid and aqueous sulfate aerosols: effect of the hysteresis of particle phase transitions, J. Geophys. Res., 113, D11206, doi:10.1029/2007jd009367, 2008.

ACPD
15, 32005–32047, 2015

Waxman, E. M., Dzepina, K., Ervens, B., Lee-Taylor, J., Aumont, B., Jimenez, J. L., Madronich, S., and Volkamer, R.: Secondary organic aerosol formation from semi- and intermediate-volatility organic compounds and glyoxal: relevance of O/C as a tracer for aqueous multiphase chemistry, Geophys. Res. Lett., 40, 978–982, doi:10.1002/grl.50203, 2013.

Xu, L., Kollman, M. S., Song, C., Shilling, J. E., and Ng, N. L.: Effects of NO_x on the volatility of secondary organic aerosol from isoprene photooxidation, Environ. Sci. Technol., 48, 2253–2262, doi:10.1021/es404842g, 2014.

Xu, L., Guo, H., Boyd, C. M., Klein, M., Bougiatioti, A., Cerully, K. M., Hite, J. R., Isaacman-VanWertz, G., Kreisberg, N. M., Knote, C., Olson, K., Koss, A., Goldstein, A. H., Hering, S. V., de Gouw, J., Baumann, K., Lee, S.-H., Nenes, A., Weber, R. J., and Ng, N. L.: Effects of anthropogenic emissions on aerosol formation from isoprene and monoterpenes in the southeastern United States, P. Natl. Acad. Sci. USA, 112, 37–42, doi:10.1073/pnas.1417609112, 2015.

Yu, K., Jacob, D. J., Fisher, J., Kim, P. S., Travis, K., Zhu, L., Yantosca, R. M., Sulprizio, M., Ryerson, T., Wisthaler, A., Fried, A., and Wennberg, P. O.: Impact of grid resolution on tropospheric chemistry simulations constrained by observations from the SEAC^{4}RS aircraft campaign, in preparation, 2015.

Zhang, H., Surratt, J. D., Lin, Y. H., Bapat, J., and Kamens, R. M.: Effect of relative humidity on SOA formation from isoprene/NO photooxidation: enhancement of 2-methylglyceric acid and its corresponding oligoesters under dry conditions, Atmos. Chem. Phys., 11, 6411–6424, doi:10.5194/acp-11-6411-2011, 2011.

Zhang, H., Parikh, H. M., Bapat, J., Lin, Y. H., Surratt, J. D., and Kamens, R. M.: Modelling of secondary organic aerosol formation from isoprene photooxidation chamber studies using different approaches, Environ. Chem., 10, 194–209, doi:10.1071/en13029, 2013.

Zhang, Q., Jimenez, J. L., Canagaratna, M. R., Allan, J. D., Coe, H., Ulbrich, I., Alfarra, M. R., Takami, A., Middlebrook, A. M., Sun, Y. L., Dzepina, K., Dunlea, E., Docherty, K., DeCarlo, P. F., Salcedo, D., Onasch, T., Jayne, J. T., Miyoshi, T., Shimono, A., Hatakeyama, S., Takegawa, N., Kondo, Y., Schneider, J., Drewnick, F., Borrmann, S., Weimer, S., Demerjian, K., Williams, P., Bower, K., Bahreini, R., Cottrell, L., Griffin, R. J., Rautiainen, J., Sun, J. Y., Zhang, Y. M., and Worsnop, D. R.: Ubiquity and dominance of oxygenated species in organic aerosols in anthropogenically-influenced Northern Hemisphere midlatitudes, Geophys. Res. Lett., 34, L13801, doi:10.1029/2007gl029979, 2007.

ACPD
15, 32005–32047, 2015

Zhu, L., Jacob, D., Mickley, L., Kim, P. S., Fisher, J., Travis, K., Yu, K., Yantosca, R. M., Sulprizio, M., Fried, A., Hanisco, T., Wolfe, G., Abad, G. G., Chance, K., De Smedt, I., and Yang, K.: Indirect validation of new OMI, GOME-2, and OMPS formaldehyde (HCHO) retrievals using SEAC^{4}RS data, in preparation, 2015.

ACPD
15, 32005–32047, 2015

Table 1. Constants for reactive uptake of isoprene SOA precursors[a].

Species[b]	H^* [M atm^{-1}]	k_{H^+} [M^{-1} s^{-1}]	k_{nuc} [M^{-2} s^{-1}]	$k_{HSO_4^-}$ [M^{-1} s^{-1}]	k_{aq} [s^{-1}]
IEPOX	3.3×10^{7}[c]	3.6×10^{-2}[d]	2.0×10^{-4}[e]	7.3×10^{-4}[e]	Eq. (2)
ISOPN$_\beta$[f]	3.3×10^{5}[g]	–	–	–	1.6×10^{-5}[h]
ISOPN$_\delta$[f]	3.3×10^{5}[g]	–	–	–	6.8×10^{-3}[h]
DHDN	3.3×10^{5}[g]	–	–	–	6.8×10^{-3}[i]

[a] Effective Henry's law constants H^* and aqueous-phase rate constants used to calculate reactive uptake probabilities γ for isoprene SOA precursors IEPOX, ISOPN$_\beta$, ISOPN$_\delta$, and DHDN following Eqs. (1) and (2). Calculation of γ for other isoprene SOA precursors in Fig. 2 is described in the text.

[b] See Fig. 2 for definition of acronyms.

[c] Nguyen et al. (2014).

[d] Cole–Filipiak et al. (2010).

[e] Eddingsaas et al. (2010).

[f] ISOPN species formed from the beta and delta isoprene oxidation channels (Paulot et al., 2009a) are treated separately in GEOS-Chem.

[g] By analogy with 4-nitrooxy-3-methyl-2-butanol (Rollins et al., 2009).

[h] Jacobs et al. (2014).

[i] Assumed same as for ISOPN$_\delta$ (Hu et al., 2011).

ACPD
15, 32005–32047, 2015

Table 2. Mean reactive uptake probabilities γ of isoprene SOA precursors[a].

Species[b]	γ	pH dependence[c]			
		pH > 3	2 < pH < 3	1 < pH < 2	0 < pH < 1
IEPOX	4.2×10^{-3}	8.6×10^{-7}	2.0×10^{-4}	1.1×10^{-3}	1.0×10^{-2}
MEPOX	1.3×10^{-4}	2.7×10^{-8}	6.4×10^{-6}	3.6×10^{-5}	3.2×10^{-4}
$ISOPN_{\beta}$	1.3×10^{-7}			–	
$ISOPN_{\delta}$	5.2×10^{-5}			–	
DHDN	6.5×10^{-5}			–	
GLYX	$2.9 \times 10^{-3,d}$			–	
MGLY	4.0×10^{-7}			–	
C_5-LVOC	0.1			–	
NT-ISOPN	0.1			–	

[a] Mean values computed in GEOS-Chem for the Southeast US in summer as sampled along the boundary-layer (< 2 km) SEAC^{4}RS aircraft tracks and applied to aqueous aerosol. The reactive uptake probability γ is defined as the probability that a gas molecule colliding with an aqueous aerosol particle will be taken up and react in the aqueous phase to form non-volatile products.

[b] See Fig. 2 for definition of acronyms.

[c] γ for IEPOX and MEPOX are continuous functions of pH (Eq. 2). Values shown here are averages for different pH ranges sampled along the SEAC^{4}RS flight tracks. Aqueous aerosol pH is calculated locally in GEOS-Chem using the ISORROPIA thermodynamic model (Fountoukis and Nenes, 2007).

[d] Daytime value. Nighttime value is 5×10^{-6}.

ACPD
15, 32005–32047, 2015

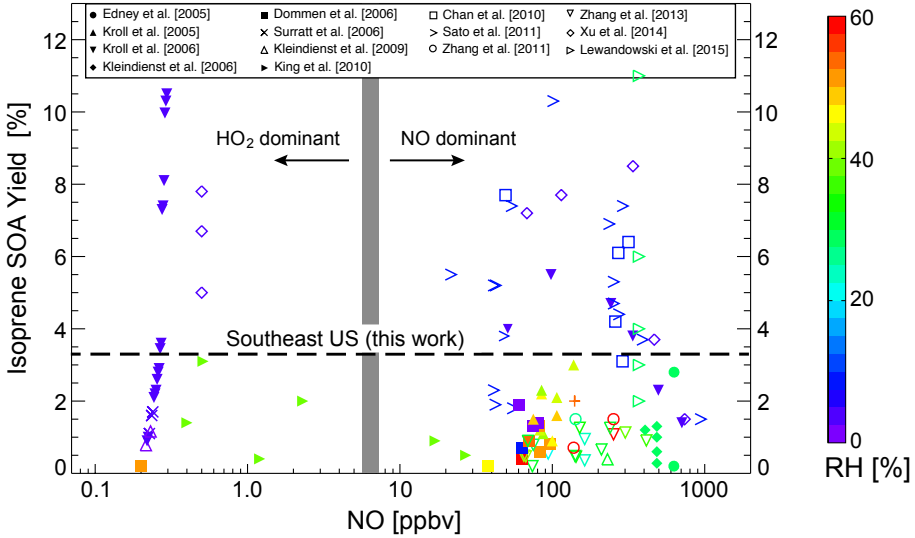

Figure 1. Yields of secondary organic aerosol (SOA) from isoprene oxidation as reported by chamber studies in the literature and plotted as a function of the initial NO concentration and relative humidity (RH). Yields are defined as the mass of SOA produced per unit mass of isoprene oxidized. For studies with no detectable NO we plot the NO concentration as half the reported instrument detection limit, and stagger points as needed for clarity. Data are colored by relative humidity (RH). The thick grey line divides the low-NO_x and high-NO_x pathways as determined by the fate of the $ISOPO_2$ radical (HO_2 dominant for the low-NO_x pathway, NO dominant for the high-NO_x pathway). The transition between the two pathways occurs at a higher NO concentration than in the atmosphere because HO_2 concentrations in the chambers are usually much higher. Also shown as dashed line is the mean atmospheric yield of 3.3 % for the Southeast US determined in our study.

ACPD
15, 32005–32047, 2015

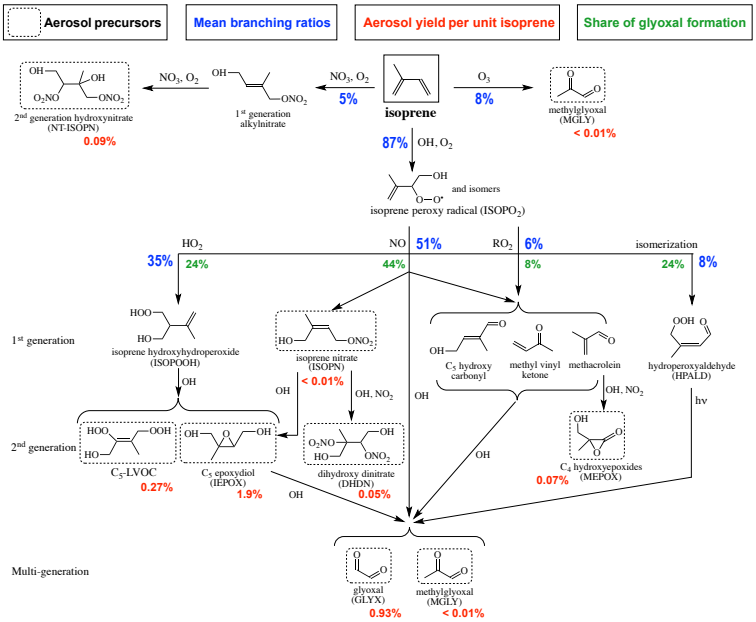

Figure 2. Gas-phase isoprene oxidation cascade in GEOS-Chem leading to secondary organic aerosol (SOA) formation by irreversible aqueous-phase chemistry. Only selected species relevant to SOA formation are shown. Immediate aerosol precursors are indicated by dashed boxes. Branching ratios and SOA yields (aerosol mass produced per unit mass isoprene reacted) are mean values from our GEOS-Chem simulation for the Southeast US boundary layer in summer. The total SOA yield from isoprene oxidation is 3.3 % and the values shown below the dashed boxes indicate the contributions from the different immediate precursors adding up to 3.3 %. Contributions of high- and low-NO_x isoprene oxidation pathways to glyoxal are indicated.

ACPD
15, 32005–32047, 2015

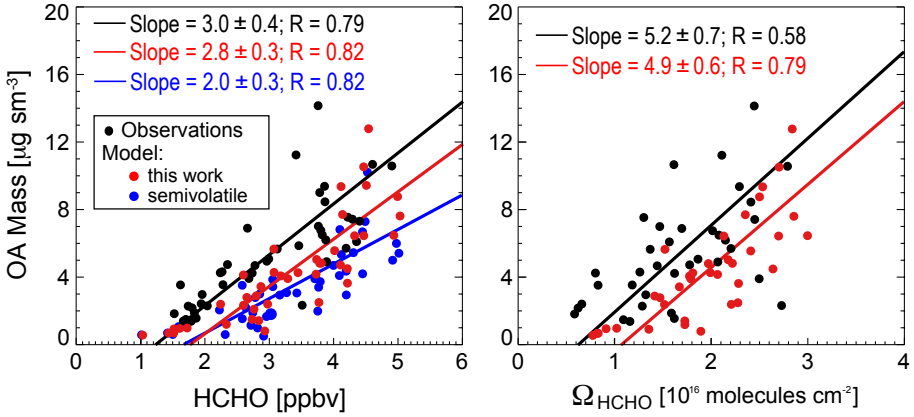

Figure 3. Relationship of organic aerosol (OA) and formaldehyde (HCHO) concentrations over the Southeast US in summer. The figure shows scatterplots of SEAC^{4}RS aircraft observations of OA mixing ratios in the boundary layer (< 2 km) vs. HCHO mixing ratios measured from the aircraft (left), and column HCHO (Ω_{HCHO}) retrieved from OMI satellite observations (right). Individual points are data from individual SEAC^{4}RS flight days (8 August–10 September), averaged on the GEOS-Chem grid. OMI data are for SEAC^{4}RS flight days and coincident with the flight tracks. GEOS-Chem is sampled for the corresponding locations and times. Results from our simulation with aqueous-phase isoprene SOA chemistry are shown in red, and results from a simulation with the Pye et al. (2010) semivolatile reversible partitioning scheme are shown in blue. Aerosol concentrations are per m^3 at standard conditions of temperature and pressure (STP: 273 K; 1 atm), denoted s m^{-3}. Reduced major axis (RMA) regressions are also shown with regression parameters and Pearson's correlation coefficients given inset. 1σ standard deviations on the regression slopes are obtained with jackknife resampling.

ACPD
15, 32005–32047, 2015

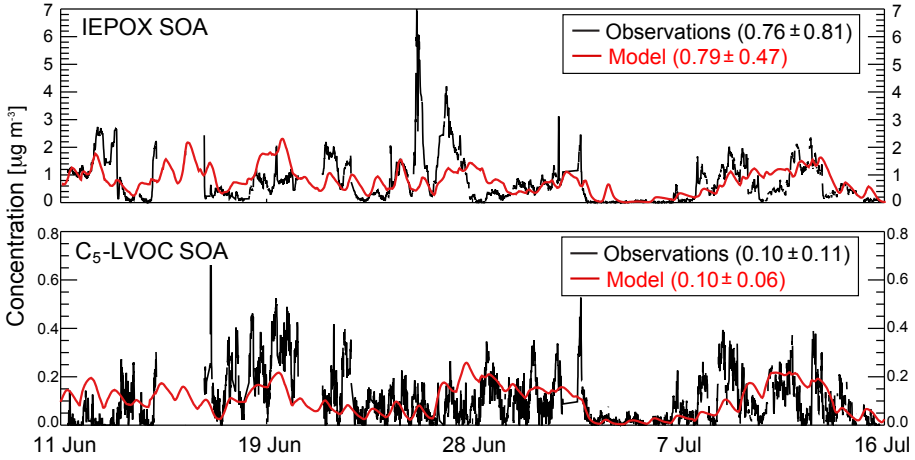

Figure 4. Time series of the concentrations of isoprene SOA components at the SOAS site in Centreville, Alabama (32.94° N; 87.18° W) in June–July 2013: measured (black) and modeled (red) IEPOX SOA (top) and C_5-LVOC SOA (bottom) mass concentrations. Means and 1σ standard deviations are given for the observations and the model.

ACPD
15, 32005–32047, 2015

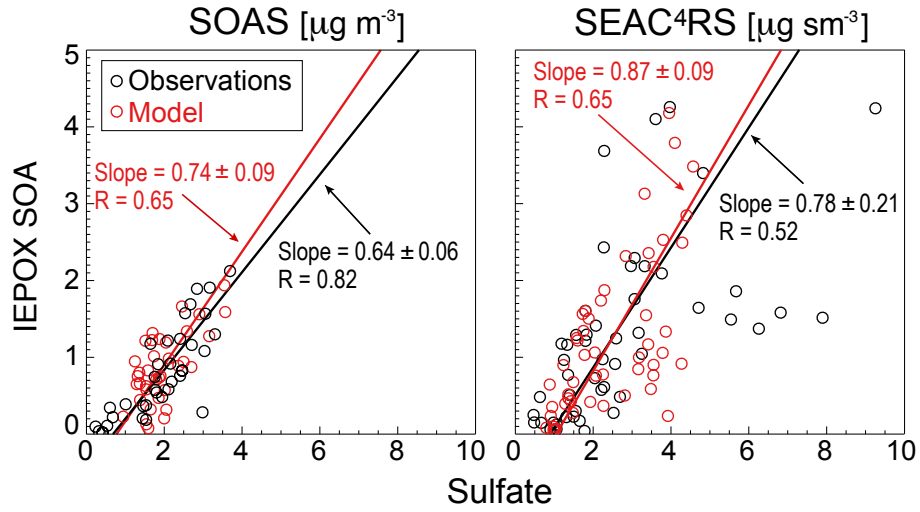

Figure 5. Relationship of IEPOX SOA and sulfate mass concentrations over the Southeast US in summer. Observed (black) and simulated (red) data are for each campaign day during SOAS (left) and in the boundary layer (< 2 km) during SEAC^{4}RS for individual flight days averaged on the GEOS-Chem grid (right). RMA regression slopes and Pearson's correlation coefficients are shown. 1σ standard deviations on the regression slopes are obtained with jackknife resampling.

ACPD
15, 32005–32047, 2015

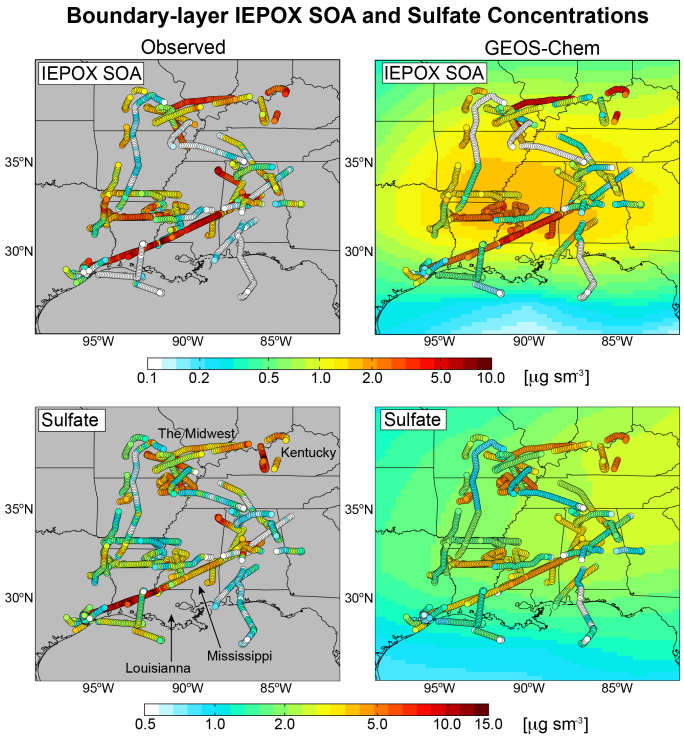

Figure 6. Spatial distributions of IEPOX SOA and sulfate concentrations in the boundary layer (< 2 km) over the Southeast US during SEAC^{4}RS (August–September 2013). Aircraft AMS observations of IEPOX SOA (top left) and sulfate (bottom left) are compared to model values sampled at the time and location of the aircraft observations (individual points) and averaged during the SEAC^{4}RS period (background contours). Data are on a logarithmic scale.

ACPD
15, 32005–32047, 2015

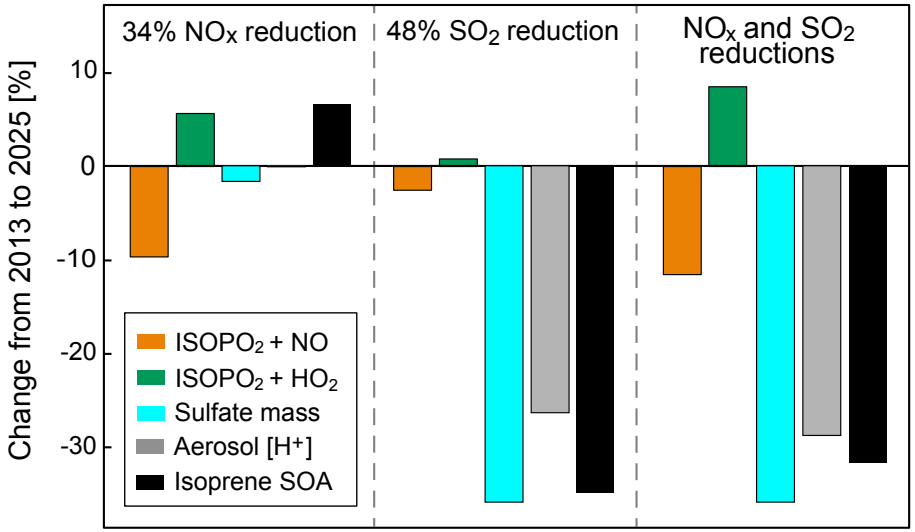

Figure 7. Effect of projected 2013–2025 reductions in US anthropogenic emissions on the formation of isoprene secondary organic aerosol (SOA). Emissions of NO_x and SO_2 are projected to decrease by 34 and 48 %, respectively. Panels show the resulting percentage changes in the branching of $ISOPO_2$ between the NO and HO_2 oxidation channels, sulfate mass concentration in $\mu g\,m^{-3}$, aerosol pH, and isoprene SOA mass concentration in $\mu g\,m^{-3}$. Values are summer means for the Southeast US boundary layer.

ACPD
15, 32005–32047, 2015